UNIVERSITÄT GREIFSWALD
Wissen lockt. Seit 1456

Schlussbericht

Umwandlungsmechanismen in Bentonitbarrieren

Kurztitel: UMB

Teilprojekt C:
Tonmineralogische Arbeiten

Carolin Podlech
Laurence Warr*
Georg Grathoff
Jörn Kasbohm

November 2019

*Korrespondenzadresse
warr@uni-greifswald.de

Dieses Projekt wurde durch das Bundesministerium für Wirtschaft und Energie (BMWi) gefördert.

Förderkennzeichen:
02 E 11344C

Das diesem Bericht zugrundeliegende Vorhaben wurde mit Mitteln des Bundesministeriums für Wirtschaft und Energie unter dem Förderkennzeichen 02E11344C gefördert. Die Verantwortung für den Inhalt dieser Veröffentlichung liegt beim Autor.

Vorhaben

Verbundprojekt UMB: Umwandlungsmechanismen in Bentonitbarrieren
Teilprojekt C: Tonmineralogische Arbeiten

Laufzeit: 01.04.2015 bis 31.12.2018

Projektleiter: Prof. Dr. Laurence Warr

Universität Greifswald
Mathematisch-Naturwissenschaftliche Fakultät
Institut für Geographie und Geologie
17489 Greifswald

Kurzfassung

Berichtsblatt

<table>
<tr><td>1. ISBN oder ISSN</td><td colspan="2">2. Berichtsart (Schlussbericht oder Veröffentlichung)
Schlussbericht</td></tr>
<tr><td colspan="3">3. Titel
Verbundprojekt UMB: Umwandlungsmechanismen in Bentonitbarrieren (UMB)
Teilprojekt C: Tonmineralogische Arbeiten</td></tr>
<tr><td rowspan="3">4. Autor(en) [Name(n), Vorname(n)]
Podlech, Carolin
Warr, Laurence
Grathoff, Georg
Kasbohm, Jörn</td><td colspan="2">5. Abschlussdatum des Vorhabens
31.12.2018</td></tr>
<tr><td colspan="2">6. Veröffentlichungsdatum</td></tr>
<tr><td colspan="2">7. Form der Publikation
Schlussbericht</td></tr>
<tr><td rowspan="3">1. Durchführende Institution(en) (Name, Adresse)
Institut für Geographie und Geologie
AG Ökonomische Geologie und Mineralogie
Universität Greifswald
Friedrich-Ludwig-Jahn Str. 17a
17489 Greifswald</td><td colspan="2">9. Ber. Nr. Durchführende Institution</td></tr>
<tr><td colspan="2">10. Förderkennzeichen
02E11344C</td></tr>
<tr><td colspan="2">11. Seitenzahl
56</td></tr>
<tr><td rowspan="3">12. Fördernde Institution (Name, Adresse)
Bundesministerium für
Wirtschaft und Energie (BMWi)
53107 Bonn</td><td colspan="2">13. Literaturangaben</td></tr>
<tr><td colspan="2">14. Tabellen
16</td></tr>
<tr><td colspan="2">15. Abbildungen
19</td></tr>
<tr><td colspan="3">16. Zusätzliche Angaben</td></tr>
<tr><td colspan="3">17. Vorgelegt bei (Titel, Ort, Datum)</td></tr>
</table>

18. Kurzfassung

Ziel der Arbeiten im Forschungsverbund war die Entwicklung abgesicherter, objektiver Kriterien zur Auswahl geeigneter Bentonite für den Einsatz in Endlagern für wärmeentwickelnde Abfälle in Tonformationen. Die tonmineralogischen Arbeiten der Universität Greifswald beinhalteten die Charakterisierung der mineralogischen und chemischen Veränderung von 1- bis 2-jährigen Bentonit-Batchexperimenten der GRS. Simuliert wurde hierbei eine Reihe von Endlagerbedingungen. So wurden die Experimente bei Temperaturen von 25, 60, 90 und 120 °C und in Kontakt mit zwei Lösungen: i) verdünnte Gipshutlösung und ii) Opalinustonlösung (beide mit bzw. ohne Zusatz mikrobiellen Substrats) durchgeführt.

Mit Hilfe von XRD, XRF, Elektronenmikroskopie (REM, TEM), spektroskopischen Methoden (EDX, IR) und der Bestimmung der Kationenaustauschkapazität (KAK) wurden die mineralogische und chemische Zusammensetzung von 15 verschiedenen Bentoniten detailliert analysiert.

Neben Austauschreaktionen mit den Lösungen zeigten die untersuchten Smektite bei Temperaturen ≤ 90 ° C keine wesentlichen Veränderungen ihrer Kationenaustauschkapazität (KAK). Detaillierte Analysen der chemischen Zusammensetzung angereicherter Smektitfraktion von 13 der 15 Bentonite mittels energiedispersiver Röntgenspektroskopie (EDX), zeigten nach Reaktion mit verdünnter Gipshutlösung bei 120 °C jedoch unterschiedlicher Grade der Schichtladungsänderung. Diese können in drei Gruppen eingeteilt werden. Gruppe A beinhaltet zwei unveränderte Na-Bentonite (B11, B23). Gruppe B besteht aus vier Ca- Bentoniten (B4, B37, B38, B49) mit geringfügigen Veränderungen, die durch einen minimalen Anstieg der negativen Tetraeder-Schichtladung gekennzeichnet sind. Gruppe C besteht aus sechs Ca-Bentoniten (B12, B13, B16, B19, B36, SD80) die einen stärken Anstieg in der negativen Tetraeder-Schichtladung und einige Veränderungen in der Oktaeder-Schichtladung aufweisen.

Die Proben SD80 (Griechenland) und B36 (Slowakei) zeigten die stärkste Änderung. Beide Bentonite wiesen eine deutlich erhöhte negativ geladene Tetraederschicht und eine geringer geladene Oktaederschicht bei 120 °C auf. Diese Veränderungen resultierten hauptsächlich aus der Substitution von Si^{4+} durch Al^{3+} in den Tetraederschichten und der Substitution von Al^{3+} durch Fe^{3+} und Mg^{2+} in der Oktaederschicht. Diese Proben zeigten zudem eine erhöhte Fixierung von K^{+} in der Zwischenschicht und erhöhte Konzentrationen von K^{+} in der umgesetzten Lösung.

Da in den Bentoniten auf mikroskopischer Ebene keine Mineralneubildung beobachtet werden konnte, sind die vorherrschenden Umwandlungsmechanismen gekennzeichnet durch Auflösung und Metallion-Substitution infolge der Wechselwirkung zwischen Bentoniten und Reaktionslösung. Ob die unterschiedlichen Grade der Smektitänderung auf die unterschiedlichen Reaktionsmechanismen zurückzuführen sind oder die heterogenen Reaktionszustände innerhalb der Batchexperimente widerspiegeln, konnte aufgrund der Komplexität der verwendeten, industriellen Bentonite in dieser Studie nicht geklärt werden.

Auch wenn die Na-Bentonite im Vergleich geringere Veränderungen zeigten als die Ca-Bentonite, kann kein einheitliches Reaktionsmodell alle experimentellen Beobachtungen erklären. Neben der unterschiedlichen Grade der Alteration, die die 15 Bentonite zeigten, konnte die Reaktionskinetik und der mikrobielle Einfluss auf das Material nicht exakt definiert werden. Für das Prozessverständnis werden einfache Experimente mit synthetischen Mineralgemischen empfohlen. Die Zugabe mikrobieller Aktivierungsmittel schien die KAK- oder Schichtladungseigenschaften der Smektitphasen über einen Zeitraum von 1 Jahr nicht zu beeinflussen. Jedoch war eine Zunahme der sulfatreduzierenden Bakterienaktivität mit der Erzeugung von Schwefelwasserstoff in Probe SD80 zu beobachten.

19. Schlagwörter

Bentonit, Montmorillonit, Schichtladung, Metallion-Substitution, Kationenaustauschkapazität, Mikroben

20. Verlag	21. Preis

Document Control Sheet

<table>
<tr><td>1. ISBN or ISSN</td><td colspan="2">2. Type of document (e.g. report, publication)

Final report</td></tr>
<tr><td colspan="3">3. Title

Joint project UMB: Alteration mechanisms in bentonite barriers

Subproject C: Clay mineralogical analyses</td></tr>
<tr><td rowspan="3">4. Author(s) (family name, first name(s))

Podlech, Carolin

Warr, Laurence

Grathoff, Georg

Kasbohm, Jörn</td><td colspan="2">5. End of project

31/12/2018</td></tr>
<tr><td colspan="2">6. Publication date</td></tr>
<tr><td colspan="2">7. Form of publication

Final report</td></tr>
<tr><td rowspan="3">2. Performing organization(s) (name, address)

Institute of Geography and Geology
Economic Geology and Mineralogy
University of Greifswald
Friedrich-Ludwig-Jahn Str. 17a
17489 Greifswald</td><td colspan="2">9. Originator’s report no.</td></tr>
<tr><td colspan="2">10. Reference no.

02E11344C</td></tr>
<tr><td colspan="2">11. No. of pages

56</td></tr>
<tr><td rowspan="3">12. Sponsoring agency (name, address)

Bundesministerium für
Wirtschaft und Energie (BMWi)

53107 Bonn</td><td colspan="2">13. No. of references</td></tr>
<tr><td colspan="2">14. No. of tables

16</td></tr>
<tr><td colspan="2">15. No. of figures

19</td></tr>
<tr><td colspan="3">16. Supplementary notes</td></tr>
<tr><td colspan="3">17. Presented at (title, place, date)</td></tr>
</table>

18. Abstract

The objective of this study was to characterize the mineralogical and geochemical changes that occurred in a set of 1 to 2 year GRS (Gesellschaft für Anlagen- und Reaktorsicherheit) bentonite batch reaction experiments that simulated a range of repository conditions relevant to storage in clay or salt host rock. The experiments investigated temperature conditions of 25, 60, 90 and 120°C and two types of water compositions: i) a saline "cap" solution and ii) an opalinus clay solution (both with and without microbial substrates).

On the basis of XRD, XRF, electron microscopy (SEM, TEM) and spectroscopic methods (EDX, IR), the mineralogical compositions of 15 types of bentonite materials were analysed in detail to determine the reaction mechanisms occurring in the batch experiments. In addition to interlayer exchange reactions with the solutions, the studied smectites were only weakly altered at temperatures ≤90°C and showed no major changes in their cation exchange capacity (CEC). However, more detailed composition analyses of purified smectite fractions of 13 of the 15 bentonites by energy dispersive X-ray spectroscopy (EDX) following reaction with the saline brine solution at 120°C did show varying degrees of layer charge alteration. These could be divided into three groups. Group A consist of two Na-bentonite samples (B11, B23) that remained unaltered. Group B comprise of four Ca-bentonites (B4, B37, B38, B49) showing minor degrees of alteration characterized by a slight increase in the negative tetrahedral layer charge. Group C consist of six Ca-bentonites (B12, B13, B16, B19, B36, SD80) with a stronger increase in the negative tetrahedral layer charge and some variations in the octahedral layer charge.

The two most altered smectites were the SD80 (from Milos, Greece) and the B36 (from Slovakia). Both samples showed notably increased negatively charged tetrahedral layers and less negatively charged octahedral layer at 120°C. These changes resulted mostly from the substitution of Si^{4+} in the tetrahedral layers by Al^{3+} and the substitution of Al^{3+} by Fe^{3+} and Mg^{2+} in the octahedral layer. These samples were also characterized by the increased fixation of K^{+} in the interlayer sites and increased concentrations of K^{+} in the reacted solution. As no microscopic signs of neocrystallization were observed in these materials, the mechanism of smectite alteration was dominated by dissolution and metal ion substitutions during water-clay interaction. Whether the different degrees of smectite alteration relate to different reaction states between the different batch experiments or reflect heterogeneous reaction states within the same batch experiment, was not resolvable in this study due to the complexities of the industrial bentonite mixtures used.

No unified reaction model appears to explain all experimental observations although the Na-bentonites are, in general, less altered than the Ca-bentonite varieties. Despite the varying degrees of alteration observed in the 15 bentonite samples studies, the reaction kinetics of bentonite mineral alteration and the precise role of microbes could not be successfully resolved and requires further experimentation using simpler, purified mineral mixtures. The addition of microbial activating agents did not appear to influence the CEC or layer charge properties of the smectite phases over a 1 year time period, but there was an associated increase in sulphate-reducing bacterial activity with the generation of hydrogen sulphide observed in sample SD80 from Milos.

19. Keywords

Bentonite, montmorillonite, layer charge, metal substitution, cation exchange capacity, microbes

20. Publisher	21. Price

Abschlussbericht (in Englisch mit deutscher Zusammenfassung)

Contents

1 Deutschsprachige Zusammenfassung

Ziel der Arbeiten im Forschungsverbund war die Entwicklung abgesicherter, objektiver Kriterien zur Auswahl geeigneter Bentonite für den Einsatz in Endlagern für wärmeentwickelnde Abfälle in Tonformationen. Die tonmineralogischen Arbeiten der Universität Greifswald beinhalteten die Charakterisierung der mineralogischen und chemischen Veränderung von 1- bis 2-jährigen Bentonit-Batchexperimenten der GRS. Simuliert wurde hierbei eine Reihe von Endlagerbedingungen. So wurden die Experimente bei Temperaturen von 25, 60, 90 und 120 °C und in Kontakt mit zwei Lösungen: i) verdünnte Gipshutlösung und ii) Opalinustonlösung (beide mit bzw. ohne Zusatz mikrobiellen Substrats) durchgeführt. Mit Hilfe von XRD, XRF, Elektronenmikroskopie (REM, TEM), spektroskopischen Methoden (EDX, IR) und der Bestimmung der Kationenaustauschkapazität (KAK) wurden die mineralogische und chemische Zusammensetzung von 15 verschiedenen Bentoniten detailliert analysiert. Neben Austauschreaktionen mit den Lösungen zeigten die untersuchten Smektite bei Temperaturen ≤ 90 ° C keine wesentlichen Veränderungen ihrer Kationenaustauschkapazität (KAK). Detaillierte Analysen der chemischen Zusammensetzung angereicherter Smektitfraktion von 13 der 15 Bentonite mittels energiedispersiver Röntgenspektroskopie (EDX), zeigten nach Reaktion mit verdünnter Gipshutlösung bei 120 °C jedoch unterschiedlicher Grade der Schichtladungsänderung. Diese können in drei Gruppen eingeteilt werden. Gruppe A beinhaltet zwei unveränderte Na-Bentonite (B11, B23). Gruppe B besteht aus vier Ca- Bentoniten (B4, B37, B38, B49) mit geringfügigen Veränderungen, die durch einen minimalen Anstieg der negativen Tetraeder-Schichtladung gekennzeichnet sind. Gruppe C besteht aus sechs Ca-Bentoniten (B12, B13, B16, B19, B36, SD80) die einen stärken Anstieg in der negativen Tetraeder-Schichtladung und einige Veränderungen in der Oktaeder-Schichtladung aufweisen. Die Proben SD80 (Griechenland) und B36 (Slowakei) zeigten die stärkste Änderung. Beide Bentonite wiesen eine deutlich erhöhte negativ geladene Tetraederschicht und eine geringer geladene Oktaederschicht bei 120 °C auf. Diese Veränderungen resultierten hauptsächlich aus der Substitution von Si4 + durch Al3+ in den Tetraederschichten und der Substitution von Al3+ durch Fe3+ und Mg2+ in der Oktaederschicht. Diese Proben zeigten zudem eine erhöhte Fixierung von K+ in der Zwischenschicht und erhöhte Konzentrationen von K+ in der umgesetzten Lösung. Da in den Bentoniten auf mikroskopischer Ebene keine Mineralneubildung beobachtet werden konnte, sind die vorherrschenden Umwandlungsmechanismen gekennzeichnet durch Auflösung und Metallion-Substitution infolge der Wechselwirkung zwischen Bentoniten und Reaktionslösung. Ob die unterschiedlichen Grade der Smektitänderung auf die unterschiedlichen Reaktionsmechanismen zurückzuführen sind oder die heterogenen Reaktionszustände innerhalb der Batchexperimente widerspiegeln, konnte aufgrund der Komplexität der verwendeten, industriellen Bentonite in dieser Studie nicht geklärt werden. Auch wenn die Na-Bentonite im Vergleich geringere Veränderungen zeigten als die Ca-Bentonite, kann kein einheitliches Reaktionsmodell alle experimentellen Beobachtungen erklären. Neben der unterschiedlichen Grade der Alteration, die die 15 Bentonite zeigten, konnte die Reaktionskinetik und der mikrobielle Einfluss auf das Material nicht exakt definiert werden. Für das Prozessverständnis werden einfache Experimente mit synthetischen Mineralgemischen empfohlen. Die Zugabe mikrobieller Aktivierungsmittel schien die KAK- oder Schichtladungseigenschaften der Smektitphasen über einen Zeitraum von 1 Jahr nicht zu beeinflussen. Jedoch war eine Zunahme der sulfatreduzierenden Bakterienaktivität mit der Erzeugung von Schwefelwasserstoff in Probe SD80 zu beobachten.

2 Summary

The objective of this study was to characterise the mineralogical and geochemical changes that occurred in a set of 1 to 2 year GRS (*Gesellschaft für Anlagen- und Reaktorsicherheit*) bentonite batch reaction experiments that simulated a range of repository conditions relevant to storage in clay or salt host rock. The experiments investigated temperature conditions of 25, 60, 90 and 120°C and two types of water compositions: i) a saline "cap" solution and ii) an Opalinus clay solution (both with and without microbial substrates). On the basis of XRD, XRF, electron microscopy (SEM, TEM) and spectroscopic methods (EDX, IR), the mineralogical compositions of 15 chemically and mineralogically diverse bentonites (6 Na-bentonites and 9 Ca-bentonites; the Na or Ca-representing the dominant cation in the smectite interlayers) were analyzed in detail to determine the reaction mechanisms occurring in the batch experiments. In addition to interlayer exchange reactions with the solutions, the studied smectites were only weakly altered at temperatures ≤90°C and showed no major changes in their cation exchange capacity (CEC). However at 120°C after 1 year, more detailed compositional analyses of purified smectite fractions did show varying degrees of layer charge alteration by energy dispersive X-ray spectroscopy (EDX). These could be divided into three groups. Group A consist of two Na-bentonite samples (B11, B23) that remained unaltered. Group B comprise of four Ca-bentonites (B4, B37, B38, B49) showing minor degrees of alteration characterised by a slight increase in the negative tetrahedral layer charge and minor increase in the negative octahedral charge. Group C consist of one Na-bentonite (B12) and five Ca-bentonites (B13, B16, B19, B36, SD80) with a stronger increase in the negative tetrahedral layer charge and larger variations in the octahedral layer charge. The remaining three Na-bentonite samples (B10, B12, B31) could not be classified due to the absence of reliable data for the smectite compositions. The two most altered smectites were the SD80 (from Milos, Greece) and the B36 (from Slovakia). Both samples showed notably increased negatively charged tetrahedral layers and less negatively charged octahedral layers. These changes resulted mostly from the substitution of Si^{4+} in the tetrahedral layers by Al^{3+} and the substitution of Al^{3+} by Fe^{3+} and Mg^{2+} in the octahedral layer. These samples were also characterised by the increased fixation of K^{+} in the interlayer sites and higher concentrations of K^{+} in the reacted solution. As no microscopic signs of neocrystallization were observed in these materials, the mechanism of smectite alteration was dominated by dissolution and metal ion substitutions during water-clay interaction. Whether the different degrees of smectite alteration relate to different reaction states between the different batch experiments or reflect heterogeneities within the same batch experiment, was not resolvable in this study due to the complexities of the industrial bentonite mixtures used. Based on previous experimentation and modelling, Fe is considered to play an important role in determining the stability of smectites. However, such reaction controls could not be recognised in this study due to the complex mineralogical and chemical variations of the bentonites studied. No unified reaction model appears to explain all experimental observations although the Na-bentonites are, commonly, less altered than the Ca-bentonite varieties. Despite the varying degrees of alteration observed in the bentonite samples studied, the reaction kinetics of bentonite mineral alteration and the precise role of microbes could not be successfully resolved and requires further experimentation using simpler, purified mineral mixtures. The addition of microbial activating agents did not appear to influence the CEC or layer charge properties of the smectite phases over a 1 year time period, but there was an associated increase in sulphate-reducing bacterial activity with the generation of hydrogen sulphide observed in sample SD80 from Milos.

Keywords: Bentonite, montmorillonite, layer charge, metal substitution, cation exchange capacity, microbes.

3 Introduction and objectives

Bentonite clay constitutes a low permeability and adsorbent material that has been proposed as one of the sealing agents for closure of underground high-level radioactive waste repository sites. Despite the many favourable properties of this material, there is a need to constrain the mineralogical reactions that may occur during saturation with varying compositions of groundwater of varying salinity at a range of repository temperatures and to assess the impact of such reactions on the long-term stability of the bentonite barrier. Such knowledge is required to select the most suitable and stable bentonite under the physical and chemical conditions relevant to geological repositories.

A key aspect of importance for maintaining the stability of the bentonite is that the smectite phases do not lose their swelling and cation adsorption capacity during progressive water-rock interaction at repository temperatures (25-120°C). In geological environments, smectite is known to undergo progressive illitization as a result of increasing temperature and K^+ activity. Prior to illitization, some intermediate precursor-illite stages have been suggested whereby the smectite is modified in terms of its layer charge and CEC properties (Kaufhold & Dohrmann 2008). Although it is clear that transition reactions can occur, the precise nature of these reactions and the controlling reaction parameters remains poorly defined. The role accessory minerals play in these reactions also remains unclear (Kaufhold & Dohrmann 2016, Warr et al. 2018).

The primary objective of this study was to determine the nature of smectite alteration for 15 industrial bentonites as part of a first step in a selection process to establish most suitable bentonite clay for application in a repository site. Reactions in two types of groundwater solution were investigated: a simulated cap rock saline brine solution (CAP) and a modelled Opalinus clay solution (OPA). In addition, a microbial substrate composed of lactate, acetate, methanol and AQDS was also added to some batches to investigate the influence of bacteria and other microorganisms. All experiments were conducted at the GRS at temperatures between 25 - 120°C and are detailed in Meleshyn (2019). The microbiological aspects are covered by Matschiavelli et al. (2019). In this study, we report the analytical results related to the onset of smectite alteration and discuss the reactions in terms of the overall mineralogy and chemistry of the bentonites. An outlook for further research is also given.

4 Experimental setup and analytical methods

4.1 Experimental setup of the batch reactors

The details of all the GRS batch reactor experiments are found in the accompanying report of A. Meleshyn (2019: 02E11344A). The key ingredients and conditions of experimentation are given in Tables 1 and 2. Eleven sets of experiments were run, each including the 15 bentonites loaded into separate reactors. The fluid: bentonite ratio by weight was set at 2:1. Reaction temperatures used were either 25°, 90° or 120°C for periods of 1 or 2 years. Sets of substrate-bearing experiments designed to simulate microbial activity were also run at 25°, 60° or 90°C for 1 or 2 years. The composition of the added substrates are given in Table 2. The University of Greifswald analyses undertaken on the materials extracted from the batch experiments are summarized in Table 1 and descriptions of the analytical procedures given in the electronic database provided (see appendix).

*Table 1: Summary of the bentonite batch reactors experiments (sets of 15) conducted at the GRS between 2015 and 2018 and the analyses made in this study. AAS = Atom absorption spectroscopy, CEC = Cation exchange capacity, EDX= energy dispersive X-ray analysis, FT-IR = Fourier-transform infrared spectroscopy, XRD = X-ray diffraction, XRF = X-ray fluorescence analysis. *only selected samples studied*

Additives	Diluted saline cap solution treated samples	Opalinus clay solution treated samples
Raw material	XRF, XRD, CEC, AAS, FT-IR, EDX	XRF, XRD, CEC, AAS, FT-IR, EDX
Without microbial substrate		
1 year batch at 25° and 90°C	XRF, XRD, CEC*, AAS*, FT-IR*, EDX*	XRF, XRD, CEC*. AAS*, FT-IR*
2 year batch at 25° and 90°C	XRF, XRD, EDX*	XRF, XRD
1 year batch at 120°C	XRD, CEC, EDX	XRD, EDX
With microbial substrate		
1 year batch at 25°C	XRF, XRD, CEC , FT-IR*	XRF, XRD, CEC, FT-IR*
1 year batch at 60, 90°C	XRF, XRD, CEC, FT-IR*	XRF, XRD, CEC, FT-IR*
2 year batch at 25°, 60 and 90 °C	XRF, XRD, EDX*	XRF, XRD

Table 2: Chemistry of the simulated groundwater solutions used for experimentation, together with the ingredients of the microbial substrate added to selective batches. AQDS = Antraquinone-2,6 disulfonate.

Additives	Diluted saline cap solution mol/L	Opalinus clay solution mol/L
pH	7.3	7.6
NaCl	2.253	0.212
$CaCl_2$	0.01	0.026
Na_2SO_4	0.008	0.014
KCl	0.0051	0.0016
$MgCl_2$	-	0.017
$SrCl_2$	-	0.00051
Substrate added to selective samples		
lactate ($C_3H_6O_3$)	0.05	0.05
Na-acetate ($CH_3COO\text{-}Na^+$)	0.05	0.05
methanol (CH_3OH)	0.003	0.003
Disodium AQDS	0.0001	0.0001

For quantitative EDX analyses of the 1 year 120°C batch, which were treated with diluted saline cap solution , we purified the bentonite samples by repeated ultrasonic dispersion and centrifugation of the <1 µm size fraction (see Appendix Podlech et al. 2018: Powerpoint presentation). This cyclic procedure was repeated at least 10 times until acceptably low traces of accessory mineral phases or their complete removal was achieved.

5 Results and discussion

The section reports on the mineralogical and geochemical analytical results of the raw and batch reacted materials. At ≤90°C only cation exchange reactions occurred in the batch experiments, whereas at 120°C after 1 year, additional metal substitutions were recognisable. Based on these results the mechanisms of smectite reaction and the controlling factors of alteration are discussed.

5.1 Mineralogy, CEC and composition of the raw bentonites

The main minerals identified in the bentonites by XRD powder analyses are listed in Table 3. Most of these samples have been well characterized in previous publications (Kaufhold & Dohrmann 2011; Ufer et al. 2008). However, due to the high degree of mineral heterogeneity reported for these bentonite sources, the mineral assemblages of the raw material used in this experimental study were restudied by quantitative XRD analyses using the Rietveld program BGMN with the PROFEX GUI (Doebelin & Kleeberg 2015).

Overall, the mineral compositions of the different bentonites vary significantly. Six of the bentonites contain 50 to 90 % Na-smectite (B9, B10, B11, B12, B13 and B23) and nine between 66-93 % Ca-smectite (B4, B16, B19, B31, B36, B37, B38, B49 and SD80) (see Table 3). Bentonites of notable purity >90 % are the B4 from Milos (92 %), the B31 sample from Armenia (92 %) and the B49 sample from Balekesir, Turkey (93 %). Notably low in smectite content is the B9 bentonite from Wyoming with just 50 %. Each bentonite sample has its own characteristic accessory mineral assemblage that totals between 7 and 50 %. All samples contain accessory quartz ranging between <1 % to 10 % and most samples show variable mixtures of alkali and plagioclase feldspar (<12 %). Only the India Kutch (B10-B12), Hungary (B13) and Bavarian bentonites (B16) appear feldspar free. Another common accessory mineral to 9 of the 15 bentonites is calcite, which ranges between <1 to 8 %. The carbonate-bearing bentonites are B9, B10, B11, B12, B13, B19, B31 (with <1 % dolomite), B38, B49 and SD80. Other notable accessory minerals detectable are pyrite (<1 %) in the Milos SD80 and gypsum (<1 %) in the B9 sample. Porous, microcrystalline, cristobalite also occurs in some bentonites, namely the Wyoming B9, the Armenia B31 and the Liskovec B36 samples. This mineral phase proved difficult to separate from purified clay mineral fractions probably due to a porous microstructure.

Table 3: *Summary of the main minerals present in the raw bentonite samples based on Rietveld analyses using Profex (Doebelin & Kleeberg 2015) and their cation exchange capacities determine by the copper triethylenetetramien (Cu(II)-trien) method (Meier & Kahr 1999). Ca-Smc = calcium smectite, Na-Smc = sodium smectite, A-Fsp = alkali feldspar, Ms = muscovite, Brt = biotite, Qtz = quartz. Ant = anatase, Cal = calcite, Hem = hematite, Rt = rutile, Ilm = ilmenite, Gt = goethite, Ap = apatite, Gp = gypsum, Mag = magnetite, Kln = kaolinite, Plg = plagioclase, Clp = clinopyroxene, Crs = cristobalite, Dol = dolomite, Sd = siderite, Chl = chlorite, Py = pyrite, CEC = cation exchange capacity.*

Sample	Source	Mineral assemblage (weight % abundance)	CEC mmol/100g
B4	Milos, Greece	Ca-Smc (92), A-Fsp (4), Brt (2), Qtz (1), Ant (<1)	94
B9	Wyoming	Na-Smc (50), Ms (22), Crs (12), Qtz (6), Plg (5), A-Fsp (3), Cal (<1), Gp (<1)	63
B10	India, Kutch	Na-Smc (90), Qtz (6), Cal (1), Ant (<1), Hem (<1), Rt (<1), Ilm (<1)	86
B11	India, Kutch	Na-Smc (82), Gt (14), Qtz (2), Ant (<2), Cal (<1)	82
B12	India, Kutch	Na-Smc (88), Ap (6), Hem (2), Gp (2), Qtz (1), Cal (1), Mag (<1)	98
B13	Hungary	Ca-Smc (84), Qtz (6), Kln (4), Cal (4), Ant (2)	73
B16	Bayern	Ca-Smc (67), Ms (24), Qtz (6), Kln (3)	58
B19	Almeria, Spain	Ca-Smc (74), Plg (12), Ms (6), Cal (2)	82
B23	Argentina	Na-Smc (80), Qtz (10), Plg (7), Alk-Fsp (3)	100
B31	Armenia	Na-Smc (92), Clp (5), Plg (2), Qtz (<1), Crs (<1), Dol (<1), Sd (<1)	80
B36	Slovakia, Liskovec	Ca-Smc (66), A-Fsp (13), Qtz (13), Crs (4), Plg (2), Chl (1), Ant (<1)	54
B37	Slovakia, Jelsovy Potok	Ca-Smc (78), Ms (6), A-Fsp (6), Plg (5), Qtz (5)	86
B38	Russia	Ca-Smc (71), Qtz (11), Cal (8), Kln (<1), Ant (<1), Plg (4) A-Fsp (4)	65
B49	Balekesir, Turkey	Ca-Smc (93), Qtz (<1), Cal (2), Plg (2), A-Fsp (2)	114
SD80	Milos, Greece	Ca-Smc (90), A-Fsp (4), Plg (2), Cal (1) Qtz (<1), Py (<1), Brt (<1), Ant (<1)	87

As expected, there is a general increase in the CEC value with increasing smectite content. Bentonite samples containing >80 % smectite have CEC's of >70 mmol/100g and bentonites with <70% smectite have CEC's of <70 mmol/100g. The most smectite-rich bentonite with 93 % Ca-smectite has the highest CEC value of 114 mmol/100g and the lowest smectitic bentonite a CEC of 63 mmol/100g.

Table 4: *Summary of the main element chemistry (% oxides) of the whole rock bentonite samples determined by XRF analysis and normalized to 100% by removal of volatile components. Bold marks highest concentrations, underlined bold mark lowest concentrations for each element.*

Sample	Source	SiO_2	Al_2O_3	MgO	Fe_2O_3	K_2O	CaO	Na_2O	TiO_2	MnO	P_2O_5
B4	Milos, Greece	62.7	20.1	3.9	9.6	0.6	**1.2**	0.8	0.9	**0.01**	0.1
B9	Wyoming	**72.4**	17.4	**1.6**	3.5	0.6	1.7	2.6	0.1	0.05	0.05
B10	India, Kutch	60.2	17.0	3.1	13.7	0.7	1.8	1.00	**2.3**	0.03	0.2
B11	India, Kutch	**50.9**	**15.2**	2.8	**24.9**	**0.2**	1.5	2.00	2.4	**0.2**	0.05
B12	India, Kutch	58.0	16.5	4.7	10.8	0.2	4.9	1.8	0.7	0.04	**2.3**
B13	Hungary	56.8	20.1	2.6	12.2	0.8	4.2	0.2	2.4	0.2	0.4
B16	Bayern	61.8	**23.3**	3.3	6.9	**2.3**	1.5	0.3	0.5	0.03	0.07
B19	Almeria, Spain	65.4	18.7	5.0	3.9	1.7	3.4	1.5	0.3	0.04	0.07
B23	Argentina	68.4	21.0	3.8	**1.1**	0.6	1.5	**3.2**	0.2	0.01	0.1
B31	Armenia	69.2	15.7	3.9	5.3	0.8	2.0	2.2	0.7	0.03	0.2
B36	Slovakia, Liskovec	66.8	18.6	1.7	8.4	1.7	1.3	0.5	0.9	0.08	0.1
B37	Slovakia, Jelsovy Potok	68.7	20.9	3.9	2.4	1.0	2.1	0.7	0.1	0.1	0.03
B38	Russia	63.9	19.3	2.9	3.6	1.3	6.6	1.3	0.8	0.1	0.2
B49	Balekesir, Turkey	66.5	18.8	**6.2**	2.1	0.4	**5.5**	0.3	**0.1**	0.1	**0.03**
SD80	Milos, Greece	63.1	21.9	3.6	5.9	1.1	3.1	**0.1**	0.9	0.1	0.2

Chemically the bentonites are characterized by variable SiO_2 concentrations between 50.9 % (B11: Indian Kutch) and 72.4 % (B9: Wyoming): see Table 4. The lowest Al_2O_3 content is also found in the B11 bentonite and the highest content in the B16 Bavarian bentonite that contains 24 % muscovite. MgO concentrations vary between 1.7 – 6.2 %, with the largest amounts found in the B49 bentonite from Turkey. Iron, measured as Fe_2O_3, important in the alteration of smectites, varies more than any other element.

The lowest concentration being 1.1% and the highest 24.9% is much higher than MgO. A characteristically low Fe-bentonite is the B23 sample from Argentina, whereas the most Fe-rich bentonites are the mafic lithologies from India (B10-B12). K_2O concentrations are generally low and range between 0.2 – 2.3 %. The CaO content is often higher than K_2O and ranges between 0.1 and 3.2 %. The largest amount of CaO is found in the B49 bentonite from Turkey. The concentration of Na_2O varies between 0.1 % (SD80 from Milos) and 2.1 % (B23 from Argentina). The oxides of TiO_2, MnO and P_2O_5 are present is low concentrations in all bentonites and range between 0.01 % and 2.3 %.

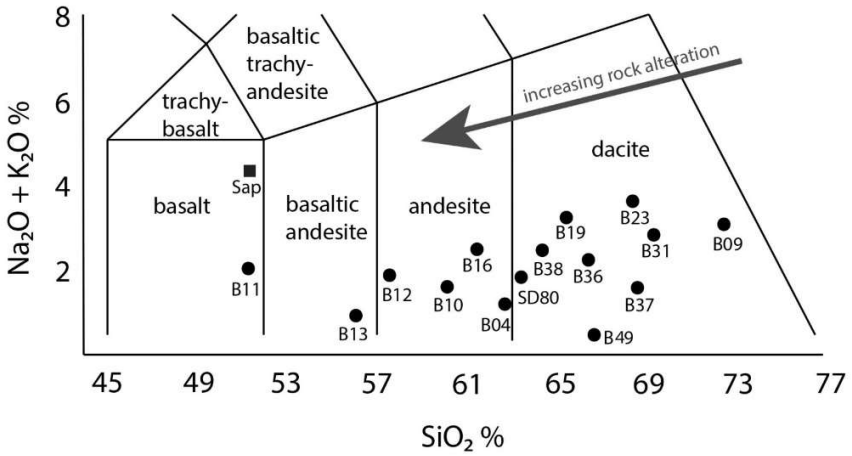

Figure 1: Igneous rock classification of the 15 bentonites using the discrimination diagram of (Le Bas et al. 1986). Increased rock alteration during formation of the bentonite often makes it compositionally more basic compared to its original protolith. Whole rock compositions determined by XRF analyses.

The bulk rock compositions of the 15 bentonite samples reflect the igneous protoliths from which the bentonites were derived as well as subsequent alteration. Such alterations can occur under marine conditions (e.g. the Wyoming B9 or Milos B4 and SD80) or by resedimentation in terrestrial environments (e.g. the Bayern B16 and Turkish B49). Nine of the bentonite samples have felsic (dacite) like compositions based on their SiO_2 and Na_2O-K_2O content (Figure 1). Four samples are more andesitic in composition and the remaining two have a basic (basaltic or basalt andesite) character. However, during the rock alteration process there are changes in composition because the more soluble cations are leached and the less soluble cations are passively concentrated, which results in more basic compositions as indicated by the arrow in Figure 1 (Christidis 1998; Warr et al. 2016).

One important variable for the materials stability may be the iron content, measured as Fe_2O_3 % (Table 4). Higher amounts of total Fe_2O_3 of the bentonites correlate with an increase in the d(060) peak of the smectite (Figure 2). Hence the bentonites with high total Fe_2O_3 also show d(060) values >1.500 Å and the bentonites of low Fe_2O_3 content have values as low as 1.496 Å.

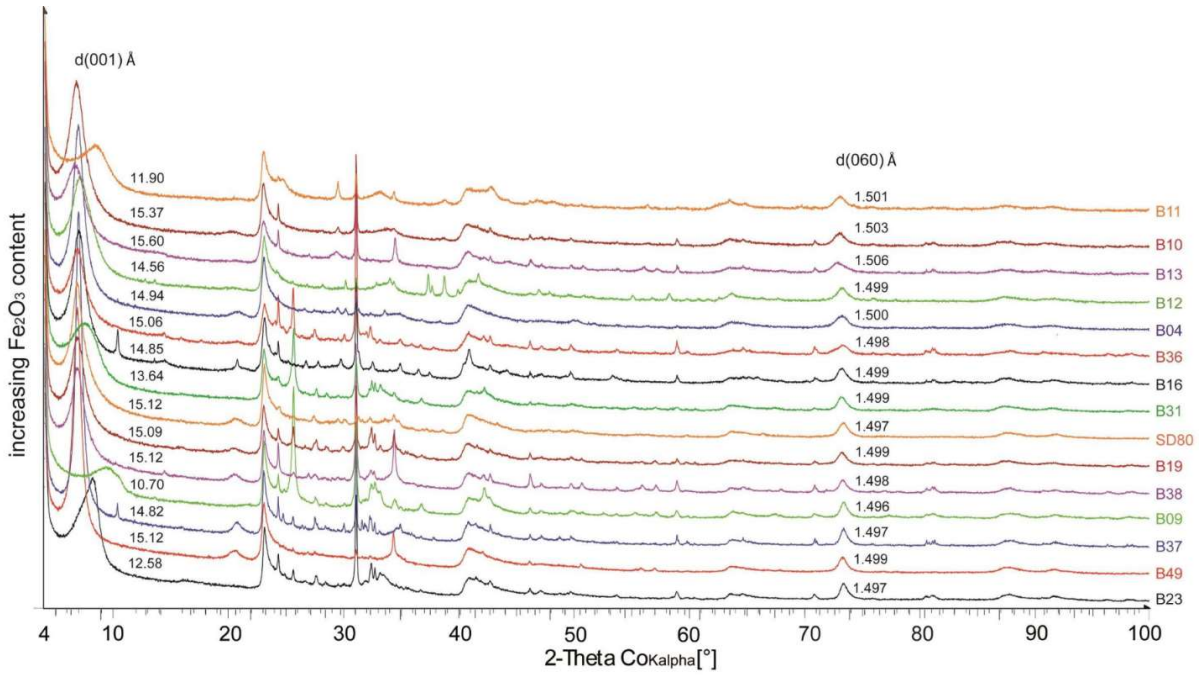

Figure 2: X-ray diffraction patterns of the 15 bentonite samples sorted according to increasing Fe_2O_3 content. The d(060) peaks show a slight shift to higher d-values with increasing Fe_2O_3.

In order to determine the interlayer cation content of the 15 bentonite samples, the cations were exchanged by the Cu(II)-trien complex and the concentrations of Na^+, K^+, Ca^{2+} and Mg^{2+} measured by F-AAS (see presentation of Podlech et al. 2016 in Appendix). Most of the samples are dominated by either Na^+ or Ca^{2+} as the main interlayer and contain minor concentrations of Mg^{2+} and K^+. The relative abundance of Na^+ and Ca^{2+} are shown in Figure 3. Five bentonite samples are dominated by the Na^+ cation (B9, B11, B12, B23 and B31), whereas the remaining 10 bentonites are Ca^{2+}-dominated. In samples B13 and B16, no Na^+ was detected in the extracted solutions following cation exchange.

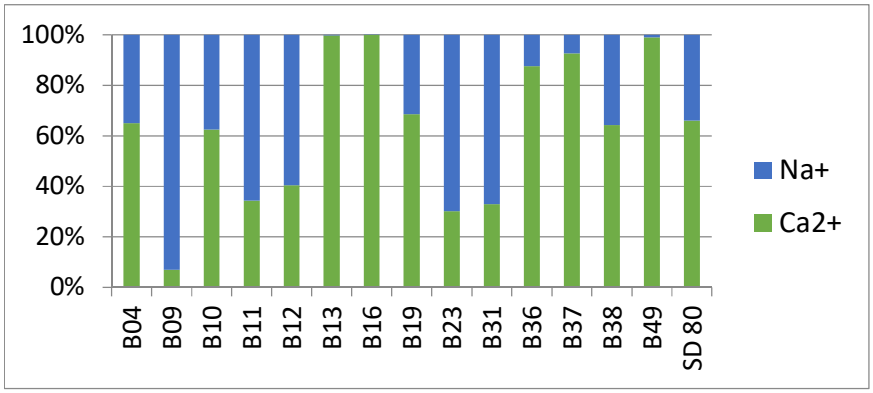

Figure 3: Relative concentrations of the interlayer cations Na^+ and Ca^{2+}, measured after cation extraction from the bentonites. Concentrations determined by atomic absorption spectroscopy.

Table 5: *Summary of the protolith lithologies of the bentonite samples, their formation conditions (if known), the dominant exchangeable cation and the experimentally determined dissolution potential in 1M NaCl (Herbert et al. 2011).*

Sample	Source	Protolith	Formation conditions	Dominant Exchangeable cation	Dissolution potential (HER 11/ in 1M NaCl
B4	Milos, Greece	Intermediate	Marine- hydrothermal?	Ca^{2+}	High
B9	Wyoming	Acidic	Marine or Na-activated	Na^{+}	High
B10	India, Kutch	Intermediate	Marine- hydrothermal?	Ca^{2+}	Low
B11	India, Kutch	Basic	Marine- hydrothermal?	Na^{+}	High
B12	India, Kutch	Intermediate	Marine- hydrothermal?	Na^{+}	High
B13	Hungary	Basic - intermediate	Unknown	Ca^{2+}	High
B16	Bayern	Intermediate	Acidic lacustrine	Ca^{2+}	High
B19	Almeria, Spain	Acidic	Acidic marine- hydrothermal	Ca^{2+}	High
B23	Argentina	Acidic	Marine- hydrothermal?	Na^{+}	Not determined
B31	Armenia	Acidic	Marine	Na^{+}	High
B36	Slovakia, Liskovec	Acidic	Nonsaline alteration?	Ca^{2+}	Not determined
B37	Slovakia, Jelsovy Potok	Acidic	Acidic lacustrine	Ca^{2+}	High
B38	Russia	Acidic	Unknown	Ca^{2+}	High
B49	Balekesir, Turkey	Acidic	Acidic lacustrine	Ca^{2+}	Not determined
SD80	Milos, Greece	Acidic	Marine- hydrothermal	Ca^{2+}	Not determined

5.2 25° and 90°C batch experiment results

4.2.1 Cation exchange capacity and layer charge determinations

Only small differences in CEC values were measured in the 1 year saline cap rock solution at 25° and 90°C experiments (Table 6). Most of these differences lie within the analytical error of the method at ca. 2 % error (± 0.85 mmol/100g). Some bentonites show a tendency toward decreasing CEC values with increasing temperatures, such as the B9 Wyoming sample and the B37 Slovakia (Jelsovy Potok) sample whereas others, such as B12 India, Kutch, yielded slightly higher CEC values at higher temperatures of alteration. Overall, these results indicate that the degree of smectite alteration in the saline solution was very small at low temperatures (<100 °C) and in most cases the differences lie within the error of measurement. The CEC values of 2 year experiments (given in Appendix) were similar to the 1 year batch samples that were studied in more detail.

Even less variability was detected in the Opalinus clay solution experiments after 1 year at 25 °C, 60 °C and 90 °C. For example, the B36 and SD80 samples produced a variability of only ± 2 mmol/100g (Table 7). Similar values were also produced after the addition of a nutrient substrate, indicating microbial activity did not change the CEC (see section 4.4). This is shown in Tables 7-9 for samples B36 and SD90 with variations of ± 1 mmol/100g.

Table 6: Cation exchange capacities (mmol/100g) for the altered bentonites in the saline cap rock solution after 1 year at 25°C and 90°C.

Sample	Source	untreated	25°C	90°C
B4	Milos, Greece	94	99	96
B9	Wyoming	63	61	60
B10	India, Kutch	86	91	87
B11	India, Kutch	82	87	82
B12	India, Kutch	98	103	105
B13	Hungary	73	79	78
B16	Bayern	58	58	56
B19	Almeria, Spain	82	76	81
B23	Argentina	100	90	96
B31	Armenia	80	70	71
B36	Slovakia, Liskovec	54	54	51
B36	Slovakia, Liskovec with substrate	54	56	53
B37	Slovakia, Jelsovy Potok	86	83	84
B38	Russia	65	63	69
B49	Balekesir, Turkey	114	120	116
SD80	Milos, Greece	87	86	87
SD80	Milos, Greece with substrate	87	85	87

Table 7: Cation exchange capacities (mmol/100g) for the altered bentonites in the Opalinus shale solution after 1 year at 25°C, 60°C and 90°C without and with a microbial substrate.

Sample	Source	untreated	25°C	60°C	90°C
B36	Slovakia, Liskovec	54	55	53	55
B36	Slovakia, Liskovec with substrate	54	56	54	56
SD80	Milos, Greece	87	88	87	89
SD80	Milos, Greece with substrate	87	86	86	87

Smectite layer charges measured using the O-D vibrational spectroscopy method (Kuligiewicz et al. 2015) in Krakow also showed no significant changes. The methodology and analyses of five of the bentonites are reported in a unpublished student report (Nietiedt 2019: see appendix) and the results summarized in Table 8 and 9.

All of the raw samples measured are characterized by layer charges that range between 0.42 and 0.56 (per O_{11}). Samples subjected to the saline cap solution with and without a microbial substrate produce values within the range of ± 0.02 and lie with the range of analytical error (< 0.02 according to Kuligiewicz et al. 2015) given for this method (Table 8). Similarly, no significant differences were observed after treatment with Opalinus clay solution after 1 and 2 years at 25 °C without and with a microbial substrate, as shown for the SD80 Milos bentonite (Table 9).

Table 8: Layer charge determination for the altered bentonites in the saline cap rock solution after 1 and 2 years at 25°C and 90°C without and with a microbial substrate.

Sample	Source	untreated	25°C-1 year	90°C-1 year	25°C-2 year	90°C-2 year
B16	Bayern	0.42	0.42	0.43	0.43	0.43
B19	Almeria, Spain	0.56	0.56	0.57	0.57	-
B36	Slovakia, Liskovec	0.41	0.40	0.39	0.41	0.42
B36	Slovakia, Liskovec with substrate	0.41	0.40	0.40	0.41	0.42
B37	Slovakia, Jelsovy Potok	0.50	0.50	0.50	0.50	0.50
SD80	Milos, Greece	0.46	0.45	0.42	0.45	0.46
SD80	Milos, Greece with substrate	0.46	0.45	0.43	0.45	0.46

Table 9: Layer charge determination for the altered bentonites in the Opalinus shale solution after 1 and 2 years at 25°C without and with a microbial substrate.

Sample	Source	untreated	25°C-1 year	25°C-2 year
SD80	Milos, Greece	0.46	0.43	0.46
SD80	Milos, Greece with substrate	0.46	0.43	0.45

4.2.2 X-ray diffraction analyses and FT-infrared spectroscopy

In addition to CEC and layer charge determinations of the 25° and 90°C sample sets subjected to saline cap and Opalinus clay solutions, the whole rock powders and clay separates were studied by XRD and FT-infrared spectroscopy in order to detect any mineralogical changes. A full list of the results are available in the electronic appendix. These results confirmed the general lack of mineralogical alteration in the 15 bentonite samples over the reaction period of 1 or 2 years. No dissolution or neoformation of minerals and no signs of smectite structural alteration were detected. The only reactions determined were changes in the interlayer cation content due to cation exchange with the reacting solution. These results are detailed below.

4.2.3 Cation exchange reactions determined by EDX measurements

Cation exchange reactions occurred in all GRS batch experiments. The nature of cation exchange is a function of the type and concentration of the exchange solution and the interlayer charge density of the smectite phase itself. An example of the cation exchange reaction is given for the B36 and SD80 bentonite samples after 2 years at 90°C in the saline cap solution (Figure 10). The B36 smectite is characterised by the exchange of Na and K with Ca, whereby K becomes the dominating interlayer cation (Figure 4a, b).

In contrast, the SD80 smectite showed exchange of Ca, Na, K, with Mg. Ca remained as the principle interlayer cation (Figure 4c,d). The exchange reactions also influence the dissolved concentrations of the reacted solution. SD80 sample solution has significantly higher concentrations of Mg than the equivalent SD80 experiments. Hence, the release of adsorbed Mg from the SD80 samples corresponded with

approximately twice the concentration of this cation in solution as measured for the B36 samples. However, it is also clear that significant amounts of Mg, Ca, Na and K were also derived from other mineral phases in these bentonites, such as from carbonates, feldspars and other phyllosilicate minerals.

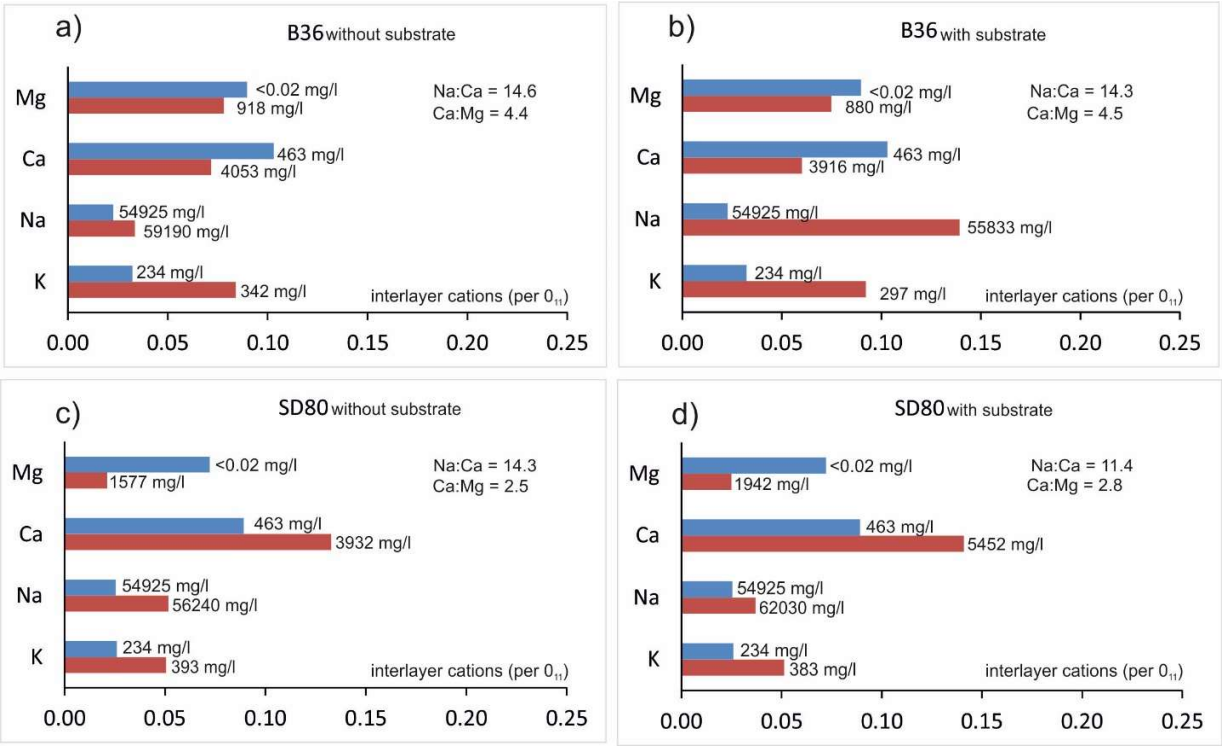

Figure 4: Smectite interlayer cation content per half unit cell (O_{11}) for the 90 °C, 2 year batch experiments with the saline cap solution. Blue bars= original unreacted state. Red bars = experimentally treated. The latter values placed at the end of each bar represent the cation concentrations in solution (results provided by A. Meleshyn, GRS). The total layer charge for the unaltered B36 and the SD80 smectites was 0.44 (per 0_{11}) and 0.37 (per 0_{11}), respectively. a) B36 without substrate, b) B36 with substrate, c) SD80 without substrate, d) SD80 with substrate.

The addition of a microbial substrate at 90°C had little effect on the exchange reactions (Figure 4b, d). Only that B36 smectite adsorbed more Na than without the substrate. The reason for this difference is not fully clear, but there is an observed difference in the layer charges between the two smectites with an increase in layer charge from 0.42 and 0.50 per 0_{11} associated with addition of the substrate. At these elevated temperatures, it is considered unlikely that any microbial activity occurred in these samples. It is more likely that the added organic acids (e.g. acetate) enhanced the alteration of the smectite, as documented in published experiments conducted at higher temperatures (Small et al. 1994). Other possibilities may be local heterogeneities in the batch reactors or the additional Na-introduced with the substrate (e.g. Na-acetate and disoldium AQDS). Further study of these effects are required.

Table 10: Interlayer cation content and layer charge determination for the altered bentonites in the saline cap rock solution after 2 years at 90°C without and with a microbial substrate.

Sample	Treatment	K	Na	Ca	Mg	Tet. charge	Oct. charge	Layer charge
B36	unaltered	0.03	0.02	0.10	0.09	-0.31	-0.13	-0.44
B36	90°C, 2 years, GH, without substrate	0.08	0.03	0.07	0.08	-0.33	-0.09	-0.42
B36	90°C, 2 years, GH, with substrate	0.09	0.14	0.06	0.07	-0.36	-0.15	-0.50
SD80	Unaltered	0.03	0.03	0.09	0.07	-0.07	-0.31	-0.37
SD80	90°C, 2 years, GH, without substrate	0.04	0.02	0.14	0.05	-0.11	-0.30	-0.41
SD80	90°C, 2 years, GH, with substrate	0.03	0.02	0.12	0.07	-0.11	-0.31	-0.42

5.3 General mineralogical, composition and layer charge characteristics

The experiments at temperatures ≤90 °C showed no significant changes in the CEC and layer charge measurements neither in the saline cap solution nor the Opalinus clay solution. Therefore we conducted more detailed microscopic and EDX-based composition determinations of the 120 °C treated samples. These samples were purified by repeated centrifugation (see section 3.1) and the quality of purification controlled from the XRD patterns of oriented, thin filmed preparations (Figure 5). Preparations were highly oriented and the measurements between 2° and 50° 2θ covered the 001 to 006 basal reflections of smectite. The purity of the mineral separates used for electron microscopy and EDX elemental analyses is summarized in Table 11 along with the smectite 001 d values in the air dried and ethylene glycolated states. During elemental mapping, any areas where impurities could be recognized were avoided (e.g. high intensity Si, Fe or Ti grains).

Table 11: Purified <1 µm montmorillonite separates, listing the occurrence of impurities in some samples. The d-values of 001 basal reflections of the smectite are shown for air dried (AD; ca. 40% relative humidity) and ethylene glycolated (GY) samples prepared as oriented thin films.

Sample	Source	Impurties	Smc 001 d-value (Å) AD	FWHM °2θ	Smc 001 d-value (Å) GY	FWHM °2θ
B4	Milos, Greece	None	14.95	0.89	16.72	0.55
B9	Wyoming	Trace of cristobalite	12.60	1.75	16.76	0.39
B10	India, Kutch	None	14.38	2.02	16.72	0.70
B11	India, Kutch	Trace of anatase	14.31	2.06	16.68	0.68
B12	India, Kutch	None	14.42	1.51	16.67	0.60
B13	Hungary	Trace of kaolinite and calcite	14.91	1.79	16.81	1.21
B16	Bayern	Trace of anatase	14.95	1.30	16.83	0.76
B19	Almeria, Spain	None	12.51	1.64	16.74	0.89
B23	Argentina	None	12.42	1.00	16.68	0.58
B31	Armenia	Trace of cristobalite	14.12	2.06	16.77	0.69
B36	Slovakia, Liskovec	Trace of kaolinite and mica	14.78	1.38	16.84	0.78
B37	Slovakia, Jelsovy Potok	None	14.83	0.79	16.64	0.42
B38	Russia	Trace of kaolinite	14.42	1.27	16.74	0.54
B49	Balekesir, Turkey	None	14.62	1.21	16.33	0.70
SD80	Milos, Greece	None	14.54	1.78	16.77	0.58

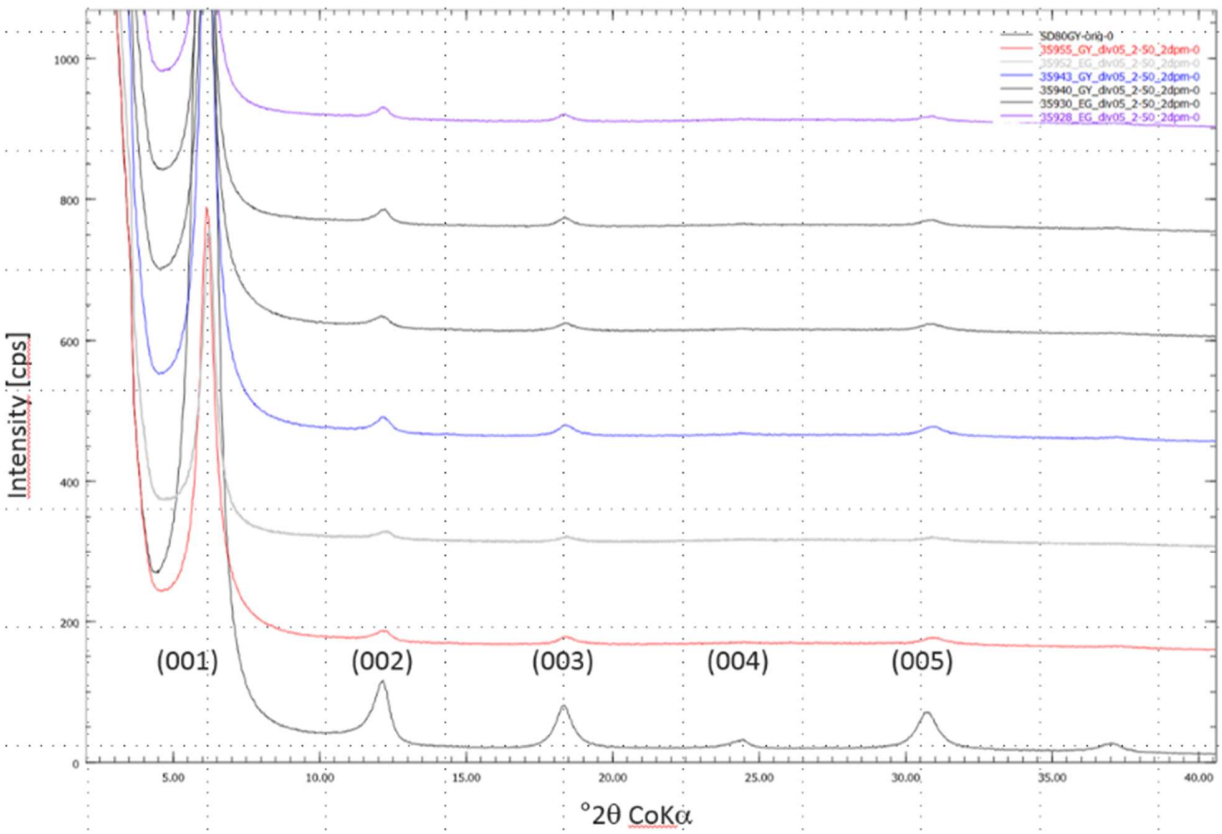

Figure 5: XRD patterns of ethylene glycolated purified (1 µm fraction) Milos SD80 bentonite in its original state (black line) and those extracted from the various batch experiments. Red = 90°C, 2 year, OPA. Grey = 90°C, 1 year, GH, blue =90°C, 2 years GH, dark grey 1 = 90°C, 1 year, GH dark grey 2 = 120°C, 1 year OPA ,purple = 120°C, 1 year GH. OPA = Opalinus clay solution. GH = "Gipshut solution (saline cap).

5.3.1 Changes in interlayer charge after treatment with CAP solution at 120°C after 1 year

Ten of the studied bentonites that were treated at 120 °C for one year showed measurable increases in the layer charge of smectite that were not evident at lower temperatures. Bentonites B9, B10 and B31 did not prove suitable for this method due to Si contamination (extremely fine grained cristobalite remained in the <1 µm fraction). Many of the increases in layer charge are small, but are reproducible and therefore considered to be significant. Based on mineral standards, the error of EDX analyses was determined to be on average 6.1 % for concentrations >1 weight% (n = 157). Following alteration, most smectites show consistent increase in tetrahedral layer charge on the order of -0.01 to -0.09 (per O_{11}) and octahedral layer charge changes ranging from +0.05 to -0.04, whereby the SD80 bentonite from Milos produced the largest difference (Table 12).

Table 12: *Smectite layer charge distributions after 120°C saline cap solution treatment after 1 year, calculated from elemental energy dispersive X-ray analyses. Stoichiometric calculations were made following published procedures (Köster 1977; Hoang-Minh et al. 2018) assuming pure dioctahedral smectites. All numerical values given represent negative charges. Bold mark changes in layer charge. *Si contamination. Δ = change, Tetra = Tetrahedral, Octa = Octahedral, Inter. = Interlayer (Tetra. + Octa.).*

Sample	Source	unaltered			120°C, 1 year			Δ	Δ	Δ	Group
		Tetra.	Octa.	Inter.	Tetra.	Octa.	Inter.	Tetra.	Octa.	Inter.	
B4	Milos, Greece	-0.22	-0.25	-0.47	**-0.24**	**-0.26**	**-0.50**	**-0.02**	**-0.01**	**-0.03**	B
B9	Wyoming*	-	-	-	-	-	.	-	-	-	
B10	India, Kutch	-0.29	-0.25	-0.54	-	-	-	-	-	-	
B11	India, Kutch	-0.26	-0.22	-0.48	-0.26	-0.22	0.48	0.00	0.00	0.00	A
B12	India, Kutch	-0.11	-0.38	-0.49	**-0.17**	**-0.39**	**0.56**	**-0.06**	**-0.01**	**-0.07**	C
B13	Hungary	-0.50	-0.11	-0.61	**-0.52**	**-0.15**	**0.67**	**-0.02**	**-0.04**	**-0.06**	C
B16	Bayern	-0.13	-0.28	-0.41	**-0.20**	**-0.26**	**0.46**	**-0.07**	**+0.02**	**-0.05**	C
B19	Almeria, Spain	-0.11	-0.48	-0.59	**-0.14**	-0.48	**0.62**	**-0.03**	**0.00**	**-0.03**	C
B23	Argentina	-0.07	-0.39	-0.46	-0.07	-0.39	0.46	0.00	0.00	0.00	A
B31	Armenia*	-0.08	-0.44	-0.36	-	-	-	-	-	-	-
B36	Slovakia, Liskovec	-0.31	-0.13	-0.44	**-0.38**	**-0.08**	**-0.46**	**-0.07**	**+0.05**	**-0.02**	C
B37	Slovakia, Jelsovy Potok	-0.07	-0.35	-0.42	**-0.08**	-0.35	**0.43**	**-0.01**	0.00	**-0.01**	B
B38	Russia	-0.16	-0.26	-0.42	**-0.17**	**0.28**	**0.45**	**-0.01**	**-0.02**	**-0.03**	B
B49	Balekesir, Turkey*	-0.00	-0.53	-0.53	-0.02	**-0.54**	**-0.56**	**-0.02**	**-0.01**	**-0.03**	B
SD80	Milos, Greece	-0.07	-0.31	-0.38	**-0.16**	**-0.29**	**-0.45**	**-0.09**	**+0.02**	**-0.07**	C

Systematic differences in tetrahedral layer charge following 120°C treatment are shown in the correlation plot of Figure 6. The best fit linear regression (R^2 = 0.95) to the tetrahedral charge of untreated versus treated samples is offset from the 1:1 line (the line of no alteration) towards more negative charges. This reflects the systematic increase in layer charge observed following alteration of the bentonite samples under these conditions. Changes in octahedral layer charge were less, with five samples showing a small increase (B4, B12, B13, B38, B4) and two samples showing a decrease (B36, SD80). These differences are represented by a good line fit (R^2=0.97) between unaltered and altered samples that fall along the 1:1 line indicative of less change (Figure 6). Only the bentonite sample B36 produced a significantly different octahedral layer charge following alteration with a change from -0.13 to -0.08 (per O_{11}). Based on these detailed compositional analyses of purified smectite we were able to divide the bentonites into three groups A, B, and C.

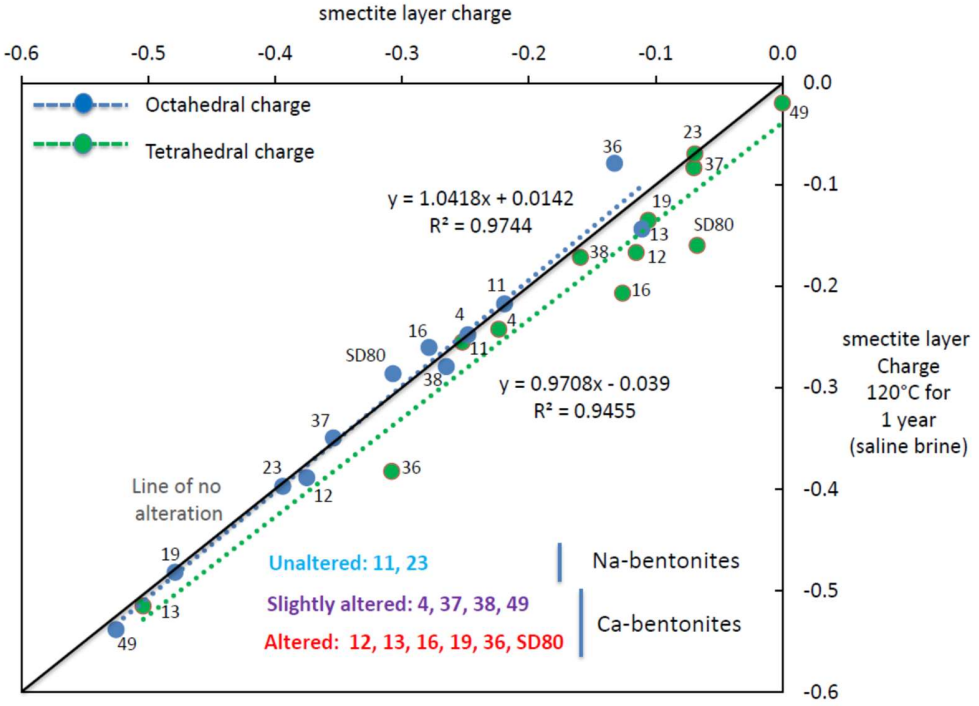

Figure 6: Correlation plot of smectite layer charge for unaltered (horizontal axis) and altered (vertical axis) samples reacted with the saline cap solution at 120°C for 1 year. The linear regression (green) for the tetrahedral charge is offset toward more negative values following alteration. The 1:1 line (solid black) matches the linear regression line (blue) for octahedral charges

5.3.2 Group A: Bentonites showing no change in layer charge

Only two of the studied bentonites showed no change in layer charge distribution when treated under the harsh conditions of 120°C for 1 year in the saline cap solution. These were the B11 (India, Kutch) and B23 (Argentina) bentonites, both of which are Na-bentonites. The difference between the smectite layer charge of the original and treated states for the B11 bentonites is shown in Table 12 and Figure 6. As the B11 bentonite has the highest Fe content (24.9 % of bulk material) and the B23 the lowest (1.1 % of bulk), it appears unlikely that the stability of these bentonites is related to the concentration of this metal. These two bentonites are of similar origin but differ significantly in composition: the Indian B11 formed by the alteration of basic volcanic ash under saline conditions with the probable influence of hydrothermal alteration (Table 5 and Shah 1997) and the Argentinian B23 bentonite formed from acidic volcanic rocks, possibly under similar conditions. The B11 and B23 bentonites have relative simple mineral assemblages of smectite, quartz, plagioclase and alkali feldspar, ± mica (Table 3). However, the basic Fe-rich composition of the B11 bentonites contains a variety of accessory phases, including goethite, anatase and calcite. Both bentonites contain no detectable pyrite by XRD. The lack of alteration for these two bentonites is not in agreement with the high solution potentials in 1M NaCl solution predicted by Herbert et al. (2011).

The absence of any change in layer charge corresponds with no major variation in the measured pH of the reacting solutions (Nietiedt 2019). The solution pH following the 1 year at 120°C for the B11 and B23 batches was 7.3 and 7.6, respectively and starting pH of the saline cap solution was 7.3. The smectites in the two samples also have similar interlayer charges of 0.47 and 0.46 (per O_{11}), respectively, although the B11 India Kutch sample has a notably higher tetrahededral charge (-0.25 per O_{11}) than that of the B23 Argentina sample (-0.07 per O_{11}). This is in accordance with a beidellite composition (octahedral Fe>Mg) for the B11 smectite (Olsson & Karnland 2009) and a montmorillonite composition (octahedral Mg>Fe) for the B23 sample (Table 12).

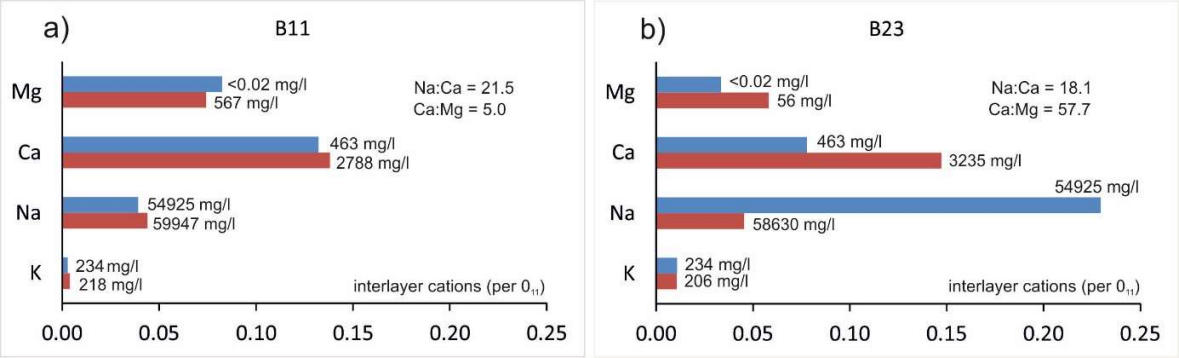

Figure 7: Smectite interlayer cation content per half unit cell (O_{11}) for the two bentonites showing no change in layer charge distribution after 1 year in the saline cap solution at 120°C. The latter values placed at the end of each bar. Blue bars= original unreacted state. Red bars = experimentally treated. The corresponding concentration of cations measured in the solution (results provided by A. Meleshyn, GRS) are given as numbers at the end of each bar (units in mg/l).

The interlayer cation content of the two smectites and the cation concentrations in solution are shown in Figure 7. The B11 smectite exchanged so few cations in this Na-rich solution suggesting minimal exchange with the solution. However, dissolution reactions in the B11 bentonite is evident. The dissolved Mg in solution increased from <0.02 mg/l to 567 mg/l. In contrast, the B23 smectite showed major change in the interlayer cation content by the exchange of Ca for Na. Significantly, both smectites contain low amounts of interlayered K and low amounts of K dissolved in the solution: a feature considered to be characteristic of the less altered bentonite materials.

5.3.3 Group B: Bentonites showing minor changes in layer charge

Four bentonite samples (B4, B37, B38 and B49) show minor changes in layer charge (Table 12, Figure 6). These samples have slightly increased negative tetrahedral charges by -0.01 to -0.02 per O_{11} with small or no variation (maxiumum of -0.02 per O_{11}) in the octahedral charge. All of these bentonites are acidic in composition (Table 2, Figure 1) and have relatively simple mineral assemblages of Ca-smectite, feldspar, quartz, ± mica and ± calcite. The Fe_2O_3 content is variable and ranges between 2.1 and 9.6 %. The B38 and B49 bentonites are notable for their high CaO content of 6.6 and 5.5 %, respectively, which reflects the higher concentrations of calcite present in these samples. Despite the small amount of alteration observed, most of these bentonites were predicted as having a high dissolution potential in 1M NaCl (Herbert et al. 2011). Most of the reacted solutions of these samples also showed little change in pH (7.0 to ca. 7.5). However, the B37 solution was a notably more acidic sample, which was measured at pH 5.9 (Meleshyn 2019).

Therefore, the small modification in the layer charge distribution of these samples shows no clear relation to the pH variation measured in the reacting solution: at least over the time period of the 1 year batch experiments.

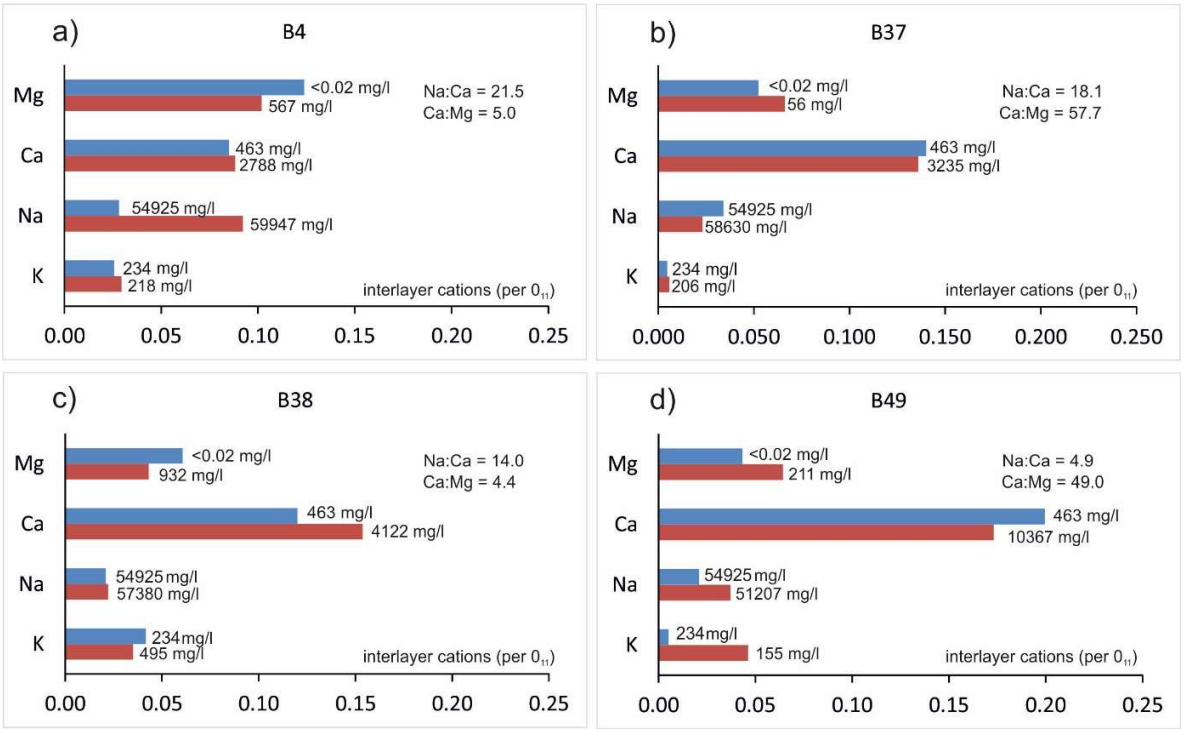

Figure 8: Smectite interlayer cation content per half unit cell (O_{11}) for the four bentonites showing only minor changes in layer charge distribution after 1 year in the saline cap solution at 120°C. The latter values placed at the end of each bar. Blue bars= original unreacted state. Red bars = experimentally treated. The corresponding concentration of cations measured in the solution (results provided by A. Meleshyn, GRS) are given as numbers at the end of each bar (units in mg/l).

The interlayer cation content of the four weakly altered smectites and the cation concentrations in solution are shown in Figure 8. All four of the smectites show only small differences the interlayer cations except for the strong uptake of Na in the B4 bentonite sample, which corresponds to the high amount of Na dissolved (59947 mg/l) in the solution and the resulting Na:Ca ratio of 21.5 (Figure 8a). In the B4 and B38 smectites, Ca was generally favoured over that of Mg, whereas the B37 and B49 smectites show Mg was favoured over Ca (Figure 8b, d). That the B4 and B38 sample solutions are characterised by a higher Mg content and Ca:Mg ratios of ≤5.0 and the B37 and B49 sample solutions by a lower Mg content and Ca:Mg ratios of >45, indicates that the preferential removal and depletion of Mg^{2+} from solution plays an important role in explaining these relationships. A similar case occurs in the behaviour of K^{+} in the B49 bentonite solution where a clear depletion from 234 to 155 mg/l occurs in association with the increase adsorption of K in the interlayer of the smectite (Figure 8d).

5.3.4 Group C: Bentonites showing larger changes in layer charge

Five bentonite samples (B12, B13, B16, B19, B36 and SD80) show larger changes in smectite layer charge (Table 12). These samples, referred to as Group C bentonites, have tetrahedral charges that are increased by -0.02 to -0.09 per O_{11}, with octahedral charges showing changes between +0.05 and -0.04 per O_{11}. The resulting interlayer charges are therefore notably higher after alteration by -0.02 to -0.07 per O_{11}.

A significant number of these altered bentonites are largely of intermediate composition and were derived from rocks of andesitic or basaltic andesite composition (Figure 1). Only the SD80 Milos and B36 bentonites are of acidic chemistry. The Fe_2O_3 content of this group is also variable and ranges from 3.9 % to 12.2 %. The K_2O varies between 0.2 to 2.3 %. This group of more strongly altered smectites are also characterized by complex accessory mineral assemblages commonly containing calcite and various types of phyllosilicate minerals, such as kaolinite (B13, B16), muscovite (B16, B19), chlorite (B38) and biotite (SD80). That four of the six bentonite samples contain calcite indicates that the buffering behaviour of calcite did not prevent the alteration of the smectite. The four bentonites containing ca. 1-2 % calcite produce saline cap rock solution pH values in the range of 7.09 to 7.3. In contrast, the two bentonites where no calcite was detected have solution equivalent pH values that are notably more acidic and range between 4.7 and 7.08. Notably acidic solutions were sampled from the B16 bentonite (pH 4.7) and the B36 bentonite (pH 4.9), whereby the source of the protons is not evident based on consideration of their mineral assemblages. One possibility is the oxidation of pyrite that could be present below the XRD detection limit. The B16 and B36 sample solutions do contain the highest levels of dissolved sulphur in solution (601 and 921 mg/l, respectively), which does support this idea.

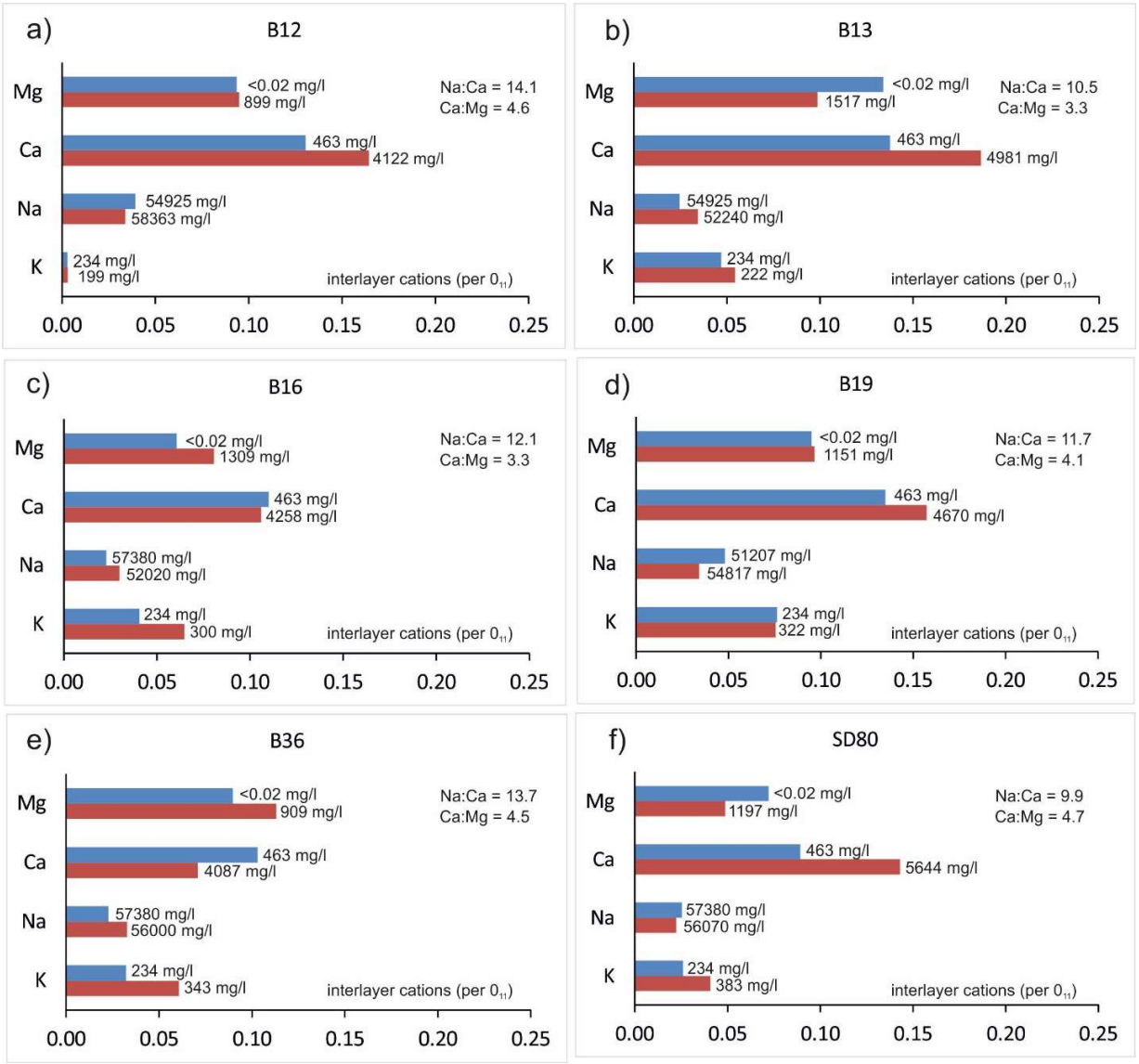

Figure 9: Smectite interlayer cation content per half unit cell (O_{11}) for the six bentonites showing larger changes in layer charge distribution after 1 year in the saline cap solution at 120°C. The latter values placed at the end of each bar. Blue bars= original unreacted state. Red bars = experimentally treated. The corresponding concentration of cations measured in the solution (results provided by A. Meleshyn, GRS) are given as numbers at the end of each bar (units in mg/l).

The cation content of the six most altered bentonites are given in Figure 9, which reveals the nature of cation exchange reactions together with changes in the solution chemistry. The most dominant exchange reaction involved the increased adsorption of Ca in the interlayer, seen in four of the six samples (Figure 9a,b,d,f). This exchange occurred largely by replacing either Na or Mg cations but the increase in Ca was also favoured by the general increase in the interlayer charge. The two exceptions to this pattern were the B16 and B36 bentonites whereby the Mg increases in the interlayer largely at the expense of Ca. Four of the bentonites also showed increased concentration of K in the interlayer, in particular in the B16, B36 and SD80 samples where the amount of dissolved K was also observed to ≥300 mgl/l in concentration (Figure 9 c,e,f). Overall, the Na:Ca and Ca:Mg ratios of the extracted solutions were surprisingly consistent and range between 9.9 -14.1 and 3.3 to 4.7, respectively.

The differences in cation exchange behaviour observed between the different bentonite samples is therefore likely to reflect the changes in layer charge distribution during alteration of the smectite.

5.4 Effects of microbial substrate addition ito the B36 and SD80 samples

Two samples, the B36 and SD80 bentonites, were analysed in more detail to establish the effects of adding microbial substrate to group C type bentonites (Table 13).

*Table 13: CEC, d(001) Å values, FWHM values and exchanged interlayer cations for the bentonite samples B36 and SD80 without and with microbial substrates. Major increase compared to raw material (20°C, no solution) shown in **bold**. Major decrease shown in **underlined bold**.*

Sample	T°C	solution	substrate	CEC mmol/100g	d(001) Å	FWHM (GY)°2θ	Na mg/l	K mg/l	Ca mg/l	Mg mg/l	Sum cations mg/l
B36	20	No	No	54.1 ± 4.1	16.9	0.9	0.5	1.1	15.0	4.2	20.8
B36	25	CAP	No	54.1 ± 1.5	17.6	0.8	0.4	0.9	15.9	4.0	21.2
B36	25	CAP	Yes	56.2 ± 4.1	17.8	1.0	**10.5**	1.0	**10.9**	**3.0**	25.4
B36	60	CAP	No	50.2 ± 1.5	17.7	0.9	**8.3**	1.0	**9.9**	**2.6**	21.8
B36	60	CAP	Yes	57.7 ± 0.7	-	-	**8.6**	0.9	**13.5**	**3.3**	26.3
B36	90	CAP	No	50.8 ± 4.5	17.6	1.0	**7.9**	1.3	**9.3**	**2.4**	20.9
B36	90	CAP	Yes	53.2 ± 5.0	17.7	0.9	**11.3**	1.0	**11.2**	**2.6**	26.1
B36	25	OPA	No	54.9 ± 3.0	17.9	0.9	0.3	0.7	16.1	4.0	21.0
B36	25	OPA	Yes	54.1 ± 3.3	17.9	0.8	0.4	1.0	14.6	4.7	20.5
B36	60	OPA	No	52.6 ± 1.7	-	-	0.9	1.0	15.8	4.9	22.6
B36	60	OPA	Yes	50.2 ± 1.5	-	-	0.8	0.9	14.9	3.5	20.1
B36	90	OPA	No	55.3 ± 2.8	17.6	0.8	**1.2**	0.8	15.2	4.7	22.0
B36	90	OPA	Yes	55.6 ± 0.4	17.8	0.8	0.5	0.9	16.1	4.8	22.3
SD80	20	No	No	86.9 ± 4.4	17.5	0.5	**10.1**	1.5	21.7	7	40.2
SD80	25	CAP	No	86.8 ± 0.9	17.5	0.5	0.9	1.1	**27.4**	6.7	36.2
SD80	25	CAP	Yes	84.6 ± 4.2	17.6	0.5	**9.6**	1.0	23.6	**5.4**	39.6
SD80	60	CAP	No	87.1 ± 1.1	17.6	0.5	**5.4**	0.9	**26.2**	**5.9**	38.3
SD80	60	CAP	Yes	86.2 ± 2.9	-	-	**6.5**	0.9	**25.8**	**6.0**	39.2
SD80	90	CAP	No	87.1 ± 1.1	17.7	0.5	**3.9**	0.9	**26.9**	**5.2**	36.9
SD80	90	CAP	Yes	84.3 ± 2.4	17.5	0.6	**11.2**	0.9	**23.7**	**5.3**	41.1
SD80	25	OPA	No	88.4 ± 3.3	17.7	0.5	**2.7**	0.9	**31.2**	6.6	41.4
SD80	25	OPA	Yes	85.7 ± 1.8	**17.1**	0.6	0.5	0.8	-	-	
SD80	60	OPA	No	86.9 ± 0.9	-	-	0.8	0.9	**28.0**	9.0	38.6
SD80	60	OPA	Yes	86.2 ± 0.9	-	-	0.3	0.8	-	-	-
SD80	90	OPA	No	88.5 ± 1.3	17.5	0.4	**1.2**	0.8	-	-	-
SD80	90	OPA	Yes	87.0 ± 1.6	**17.0**	0.7	0.5	0.8	**26.6**	9.0	36.8

No significant differences in the CEC values can be observed in any of the experiments used to test the effects of adding the microbial substrate (Table 13). All of the B36 samples without and with a substrate fall within the range of error determined on the untreated B36 raw material (54.1 ± 4.1 mmol/100g). Adding the substrate to the saline cap solution B36 samples did significantly influence the cation content of the smectite with the exchange of Ca^{2+} and Mg^{2+} by Na^{+} derived from the addition of sodium acetate, disodium AQDS-sodium and sodium lactate. Such an exchange, however, was not observed in the Opalinus clay solution treated materials where bivalent cations (Ca^{2+} and Mg^{2+}) continued as the dominant interlayer cations. The larger differences in CEC values seen for the 60°C and 90°C B36 samples reacted in the saline cap solution are also not considered to be significantly different when considering the errors of analyses involved. For the B36 sample set there is also no obvious change in the d(001) Å and FWHM (GY)°2θ values that would indicate smectite alteration or the permanent loss of swelling (Table 13, Figure 11).

A consistent pattern of results was also observed for SD80 bentonite samples without and with substrate. Only cation exchange reactions are evident with Na^+ derived from the substrate replacing Ca^{2+} and Mg^{2+} in the interlayers of the smectite in the saline cap solution experiments and Ca^{2+} and Mg^{2+} dominating the smectite interlayers in the Opalinus clay solution. The later effect can be attributed to the higher Ca:Na ratio of the Opalinus solution (ca. 0.11) compared to that of the saline cap solution (Ca:Na ratio ca. 0.004).

Based on these results, any microbial activity that may have occurred in these samples does not appear to have influence the CEC of the smectite phases in these samples and the changes in cation content can be attributed to the change in solution chemistry caused by addition of the substrate compounds. This observation is in accordance with the lack of any changes in layer charge reported in these sample (Table 13).

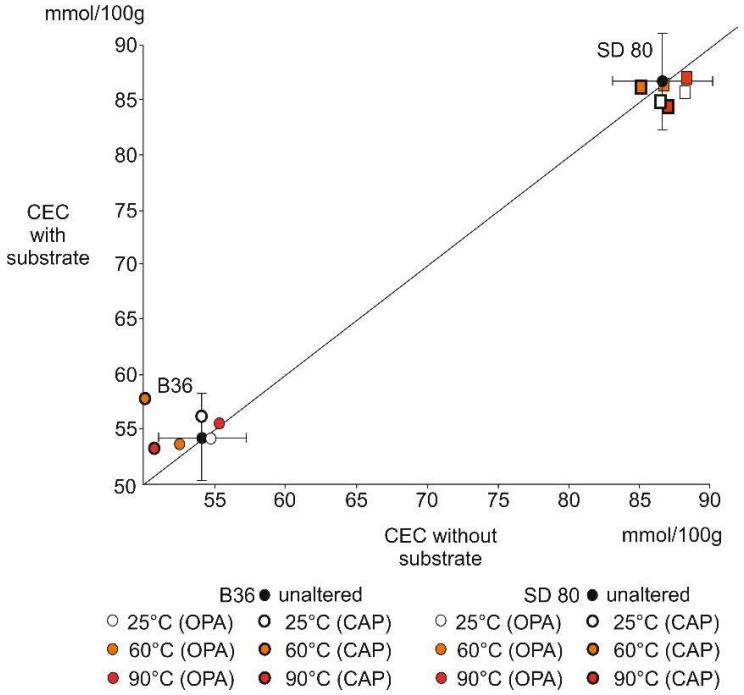

Figure 10: CEC of the B36 and SD80 samples without and with the addition of the microbial substrate.

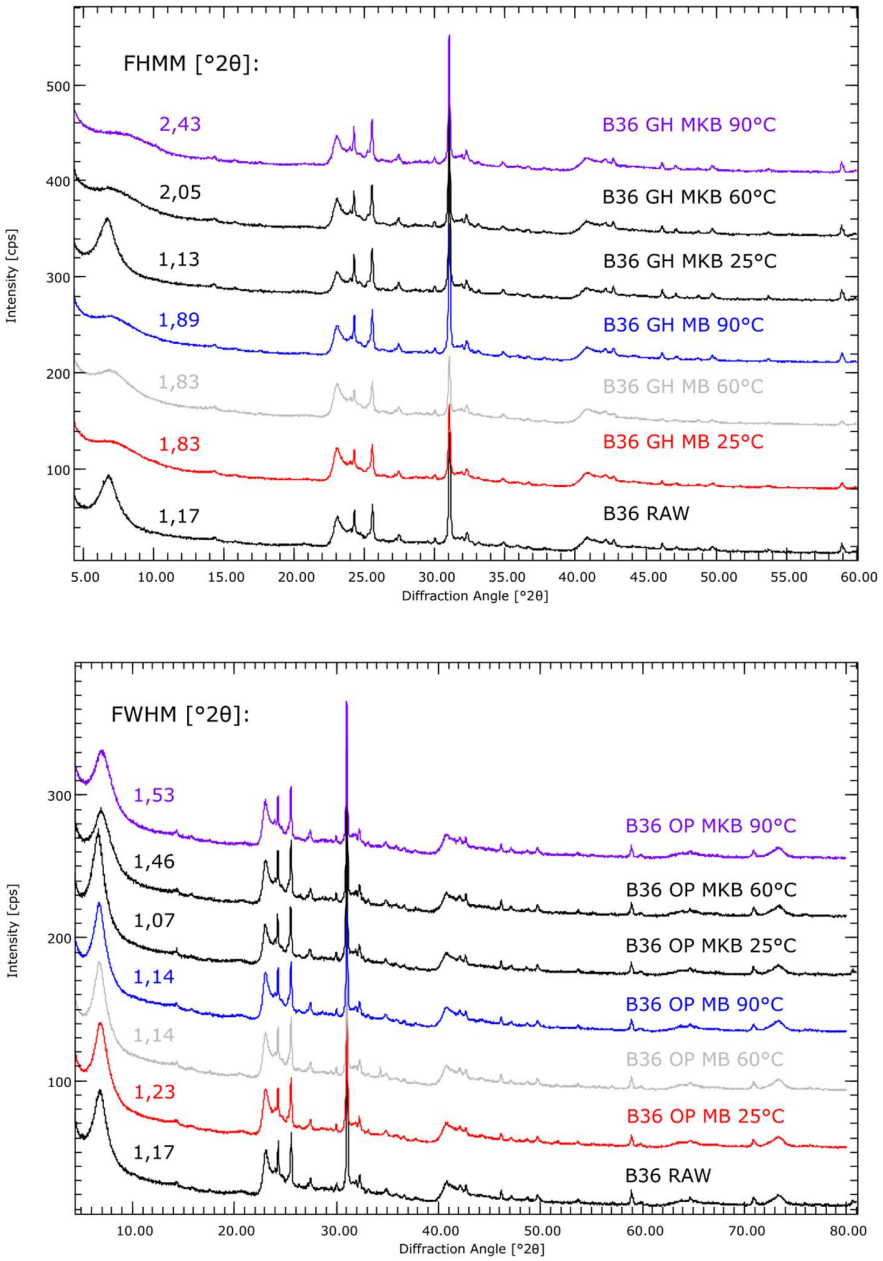

Figure 11: XRD of the sample B36 with and without the addition of the microbial substrate, reacted in CAP and OPA solution.

Despite the general lack of permanent alteration of the smectite in the B36 and SD80 samples, some significant differences could be recognised in the swelling behaviour seen in the XRD patterns of naturally dried samples that require explanation. Random powder XRD of washed B36 samples show significant d(001) Å peak broadening and loss of intensity following treatment in the saline cap solution (Figure 11). These changes can be largely attributed to the cation exchange reactions that occurred during experimentation whereby the replacement of bivalent cations by Na leads to a shift and broadening of the d(001) reflection due to the delamination of particles into smaller thicknesses. These changes are recognizable in the bentonite without and with the addition of the substrate.

Similar changes towards broader, less intense reflections with smaller d(001) values are also notable in the SD80 samples treated with saline cap solution that are characterised by Na-exchange, practically the higher temperature experiments of 60° and 90°C without the addition of substrate (Figure 12). The higher concentrations of Ca and Mg in the interlayers of the SD80 smectite reaction in Opalinus clay solution are also clearly seen by the sharper reflections d(001) ca. 15 Å reflections indicative of the thicker X-ray scattering particle thicknesses that result from the dominance of bivalent interlayer cations.

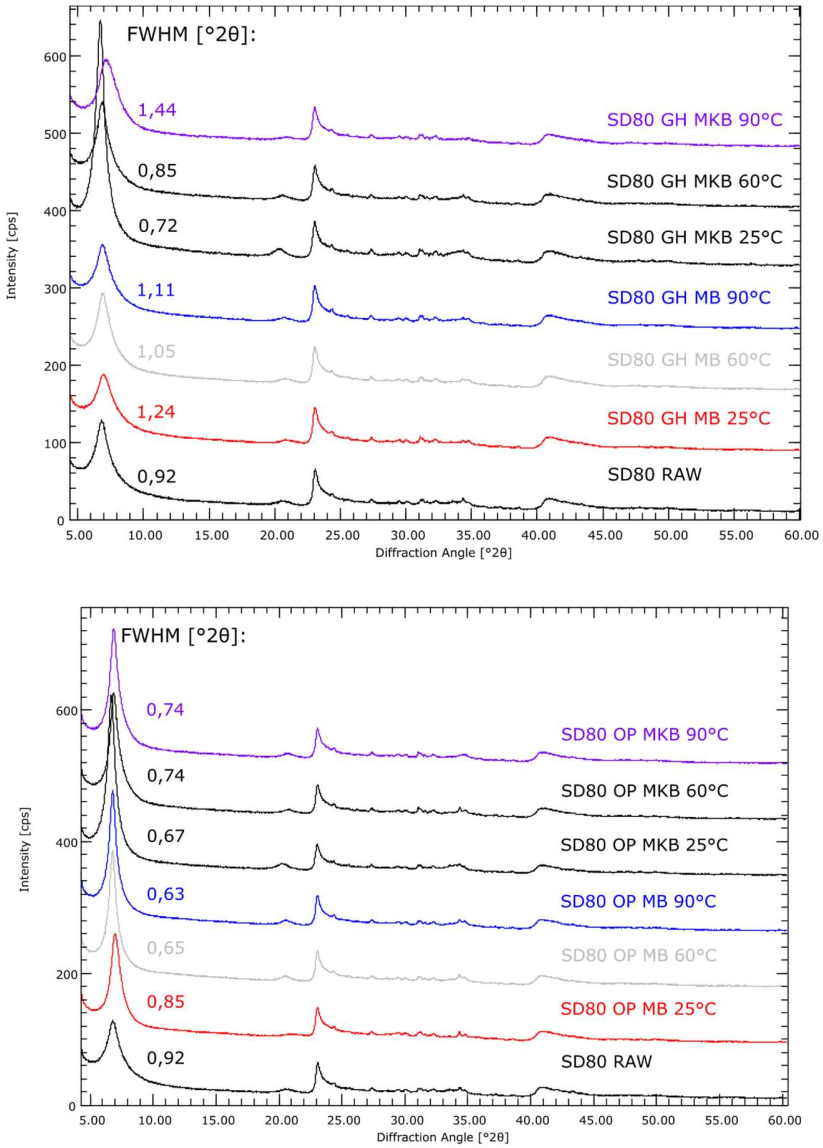

Figure 12: XRD of the sample SD80 with and without the addition of the microbial substrate, reacted in CAP and OPA solution.

In order to test the reversibility of these changes in swelling, the untreated B36 raw material and a reacted B36 sample subjected to saline cap solution for 1 year at 90°C were exchanged with 1N $SrCl_2$ and reanalysed by XRD.

After Sr-saturation, there were not more differences observed between the raw and reacted materials in terms of their peak position, Full-width-at-half-maximum (FWHM) and maximum intensities (Table 14). The similarities in the smectite apply to both air-dried and ethylene glycolated when treated with $SrCl_2$ solution and washed. This indicates that the apparent differences in XRD reflections of smectites observed in the various experiments (Figure 11, 12) are largely a function of cation exchange reactions.

Table 14: X-ray diffraction results for the B36 sample showing differences in the d(001) values and their Full-Width at-Half-Maximum (FWHM) values.

No.	$SrCl_2$	oP	T [°C]	Duration [a]	Solution	d(001) [Å]	FWHM (001) [°]	max. I (001) [cps]
B36-raw	no	Air-dried	20	0	-	12.9	2.0	78
B36-raw	yes	Air-dried	20	0	-	14.8	1.4	300
B36-raw	yes	Glycolated	20	0	-	16.8	0.8	240
SD80 OPA 90°C without substrate	yes	Air-dried	90	1	CAP	14.8	1.7	130
SD80 OPA 90°C without substrate	yes	Glycolated	90	1	CAP	17.1	0.9	190

In order to visually exam the effects of adding a microbial substrate on the smectite and bacterial assemblages, direct observations by SEM where made (Figure 13). The left image of Figure 13 represents a secondary electron image of the bacterial cell which is about 4 µm in length. Small, platy particles of smectite are seen attached to the bottom of the cell and the Si mapping reveals the location of other smaller smectites. The organic nature of the cell is seen clearly in the C map and the location of phosphatic bodies within the cell shows up on the map of P. These bodies are likely to represent cellular globules used to sequester metals present in the surrounding solutions (Warr et al. 2009). These observations confirm there is a close relationship between bacterial cells and smectite particles in the materials studies and that some of the bacteria have the ability to sequester metals as a mechanism of self-protection. No obvious traces of biofilm was observed in the samples studies.

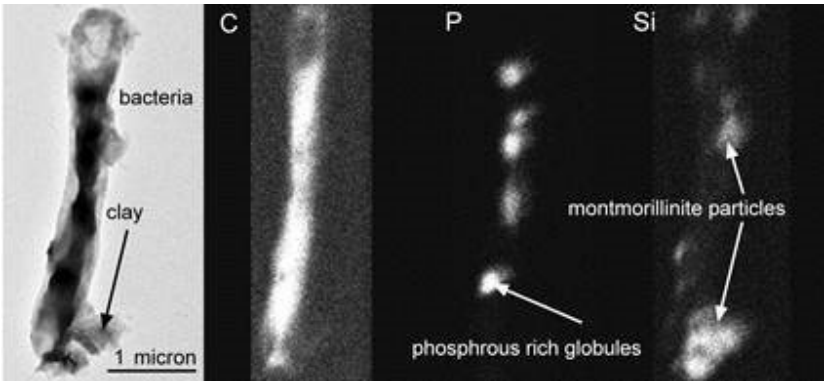

Figure 13: SEM secondary electron image and elemental maps (C, P, S) of a bacterial cell with smectite clay minerals attached. The P spots represent phosphatic bodies found with the cell.

5.5 Hydration behaviour of the SD80 bentonite

The hydration behaviour of the SD80 bentonite from Milos was studied in detail using in situ "wet cell" X-ray diffractometry (Warr & Berger 2007). This bentonite was selected as it represents one of the most reactive (group C) materials studied and contains detectable concentrations of calcite (ca. 1%). Two wet-cell experiments were prepared using the raw SD80 bentonite powder, which was loaded into the cells with packing densities of ca. 1.5 g/cm^3. Details of the experimental setup are provided by Manzel (2019; included in the appendix).

The two cells were slowly hydrated for 57 days by connection to Teflon bottles containing 50 ml of solution. Wet cell 1 was hydrated with the Opalinus clay solution and wet cell 2 with the saline cap solution (Table 2, Figure 14). The cells were stored vertically so that the solution percolated slowly into the chamber by gravity via small 2 mm holes. Although the cells do allow for the complete percolation of water, with holes on each side, no flow-through was observed in these experiments and the collecting bottle at the base of the cell remained empty.

During water inflow, the state of smectite hydration during the first two weeks was determined by daily measurement of each cell by XRD. After this period, the cells were measured weekly until complete hydration was observed. The weight of the cells were also monitored to determine the amount of inflowing water (Figure 15). The water intake during the first 100 hours of hydration was rapid and consistent for both wet cells with ca. 0.1 g/g entering in the bentonite powder. After this time period, the saline cap and Opalinus clay solution then entered the cell at a slower rate until no more inflow was observed after 600 hours. The slight decrease in the amount of water in the saline cap solution treated bentonite sample after 600 hours of hydration indicates the rate of evaporation from the cell is higher than the rate of inflow.

Figure 14: X-ray diffraction monitoring of the hydration of SD80 bentonites at 25°C in (left, wetcell1) Opalinus clay solution and (right, wetcell2) saline cap solution.

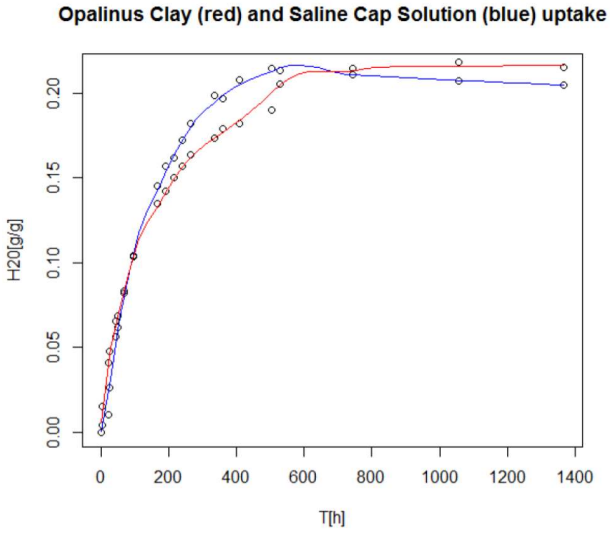

Figure 15 Weight of H_2O flowing into the cell during hydration of SD80 bentonites at 25°C in () Opalinus clay solution (red) and saline cap solution (blue).

The state of saturation could also be assessed from the appearance of the hydrated bentonite XRD patterns (Figure 16).

Based on the shape of the 001 smectite reflections, both are considered to represent mixtures of at least 3 types of water-layer structures with thicknesses of 12.4 Å (1-water-layer), 15.1 Å (2-water-layers) and 18.5 Å (3-water-layers). Small amounts of a fourth water-layer may also occur at 20.2 Å in strongly hydrated samples.

The rate of SD80 hydration was notably faster in Opalinus clay solution than in the saline cap solution. This can be seen by the shift in the 001 smectite reflection from ca. 15.3 Å (a 2 water layer structure) to 18.6 Å (a predominantly 3 water layer structure: see Figure 16). This change occurred within the first ten days of water intake. In contrast, more limited interlayer hydration occurred in the saline cap solution whereby the 2 water-layer structure remained predominant throughout the period of hydration.

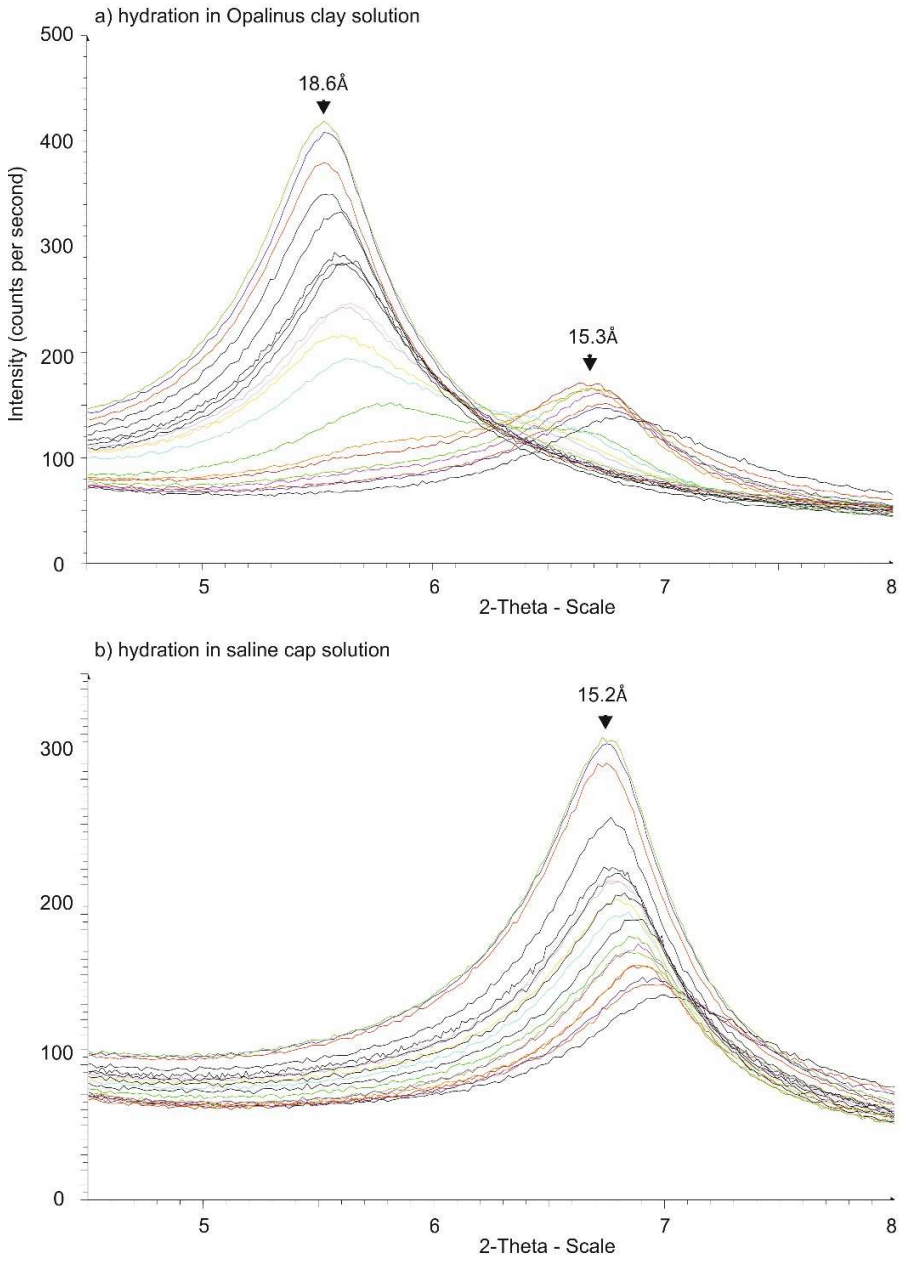

Figure 16: X-ray diffraction results of the progressive hydration of the SD80 bentonite at 25°C in a) Opalinus clay solution and b) saline cap solution.

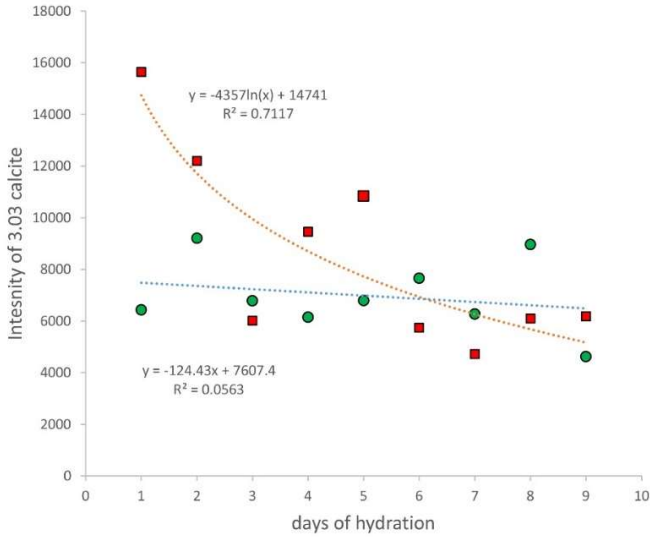

Figure 17: Change in the intensity (counts per second) of the 3.03 Å calcite reflection in the SD80 bentonite during hydration with a) saline cap solution (red squares) and b) Opalinus clay solution (green circles) at 25°C.

In addition to the changes in smectite hydration state, the intensity of the 3.03 Å calcite reflection in the SD80 bentonite samples was used to study the dissolution of this carbonate mineral phases at 25 °C. Despite the strong fluctuation in the reflection intensity measured, which can be attributed to textural changes occurring at the top of the sample during swelling, there was a significant decrease in the intensity of the calcite reflections with time when treated with the saline cap solution (Figure 17). The decrease in intensities could be well fitted with a natural logarithmic curve (R^2 = 0.72), with a decrease from ca. 16000 counts to ca. 7000 counts occurring over the first 10 day duration of fluid-bentonite interaction. As the starting concentration of calcite was determined to be 1 weight% determined by Rietveld analyses (Table 3), the dissolution of calcite can be estimate to reduce the amount of calcite in the sample by over 0.5 weight%. In contrast to the saline cap solution, no major dissolution and reduction in the intensity of the 3.03 Å calcite reflection occurred in the Opalinus clay solution. As the starting pH of the saline cap and Opalinus solutions were similar (7.4 and 7.6, respectively), it appears unlikely that the pH is the main controlling factor as to why significantly more calcite was dissolved in the more saline solution. This experimental difference is more likely to reflect the differences in salt concentration, whereby an increase concentration of NaCl in solution leads to an increase in the solubility of $CaCO_3$ (Berkowitz et al. 2003). In this case, the diluted saline cap solution has a NaCl concentration that is over ten time higher than the Opalinus clay solution and therefore the calcite can be expected to be considerably more soluble in the saline solution experiment at 25°C.

5.6 Mechanism of smectite alteration

Based on our results for the GRS batch reactor experiments, clear signs of smectite alteration were evident in the saline cap solution at temperatures of 120 °C following 1 year of reaction time. At conditions ≤90 °C, none of the batch experiments showed indications of such alteration, suggestive of a high degree of stability over the 2 year time period tested. The principle mechanism of clay mineral alteration observed at elevated temperatures occurred by substitution of metals in the tetrahedral sheets of the different smectites with the exchange of Si^{4+} by Al^{3+}. This type of substitution could be recognized in 10 of the 12 bentonites studied in detail and resulted in an increase in the charge of the tetrahedral sheet by -0.01 to -0.09 per O_{11} (Table 14). This type of reaction was the main mechanism by which the interlayer charge increased during smectite alteration in the saline cap solution under the elevated temperature.

Table 15: *Changes (**Δ**) in layer charge properties (per O_{11}) between unaltered and altered smectites after treatment with saline cap solution at 120°C and 1 years. Tetra. = Tetrahedral, Octa. = Octahedral, Inter. = Interlayer. The mechanisms of metal substitution detected by EDX analyses is also listed, as well as the pH of the reacted solutions (provided by A. Meleshyn, GRS). *indicates pH values taken from the 90°C, 2 year series of experiments. Inter. = total change in layer charge. Group A indicate no change in interlayer charge. Group B is defined by small differences in tetrahedral charge of either -0.01 or -0.02 and accompanied by octahedral charges differences in the range of 0 to -0.03. Group C represent larger changes in tetrahedral charge between -0.02 and -0.09 and for octahedral charges between -0.04 to +0.05*

Sample	Source	Δ	Substitution	Δ	Substitution	Δ	pH	Group
		Tetra.	Tetra.	Octa.	Octa.	Inter.		
B4	Milos, Greece	**-0.02**	Si^{4+} by Al^{3+}	**-0.01**	Al^{3+} by Fe^{3+} and Mg^{2+}	**-0.03**	3.65*	B
B9	Wyoming*	-	-	-	-	-	7.52*	
B10	India, Kutch	-	-	-	-	-	6.82*	
B11	India, Kutch	0.00	No exchange	0.00	No exchange	0.00	7.32	A
B12	India, Kutch	**-0.06**	Si^{4+} by Al^{3+}	**-0.01**	Al^{3+} by Fe^{3+} and Mg^{2+}	**-0.07**	7.28	C
B13	Hungary	**-0.02**	Si^{4+} by Al^{3+}	**-0.04**	Fe^{3+} by Mg^{2+}	**-0.06**	7.08	C
B16	Bayern	**-0.07**	Si^{4+} by Al^{3+}	**+0.02**	Fe^{3+} and Mg^{2+} by Al^{3+}	**-0.05**	4.69	C
B19	Almeria, Spain	**-0.03**	Si^{4+} by Al^{3+}	**0.00**	No exchange	**-0.03**	7.2	C
B23	Argentina	0.00	No exchange	0.00	No exchange	0.00	7.56	A
B31	Armenia*	-	-	-	-	-	7.37	-
B36	Slovakia, Liskovec	**-0.07**	Si^{4+} by Al^{3+}	**+0.05**	Fe^{3+} and Mg^{2+} by Al^{3+}	**-0.02**	4.89	C
B37	Slovakia, Jelsovy Potok	**-0.01**	Si^{4+} by Al^{3+}	0.00	No exchange	**-0.01**	5.89	B
B38	Russia	**-0.01**	Si^{4+} by Al^{3+}	**-0.02**	Al^{3+} by Fe^{3+} and Mg^{2+}	**-0.03**	7.08	B
B49	Balekesir, Turkey*	**-0.02**	Si^{4+} by Al^{3+}	**-0.01**	Al^{3+} by Fe^{3+} and Mg^{2+}	**-0.03**	7.33	B
SD80	Milos, Greece	**-0.09**	Si^{4+} by Al^{3+}	**+0.02**	Al^{3+} and $Mg^{2+}$by Fe^{3+}	**-0.07**	7.09	C

The nature of metal substitutions in the octahedral sheets of smectites is observed to be more complex. Weakly altered bentonites (group B) are generally characterized by a slightly more negative octahedral layer charge attributable to the substitution of Al^{3+} by Fe^{3+} and Mg^{2+} (Table 14). The difference in charge is small and ranges between -0.01 to -0.02 per O_{11}. Group C bentonites show more diverse types of octahedral metal substitutions and in three samples (B16, B36 and SD80) a relative decrease in charge occurred by replacement of Mg^{2+} by Al^{3+} or Fe^{3+}. Despite the complexity of octahedral metal substitutions, all altered bentonites samples are recognizable by a relative increase in layer charge by -0.01 to -0.07 per O_{11}. This increase in charge explains some of the changes in interlayer cation content, in particular the increase of K^+ adsorbed from the reactive solution. Although there is no direct correlation between the amount of K^+ adsorbed in the smectite interlayers and the concentration of dissolved K^+ in solution, there is clear power law correlation between the K^+ adsorbed in the smectite interlayer and the K^+ solution : K^+ interlayer ratio (Figure 18). This relationship indicates that batch experiments containing smectites with low amounts of K^+ in the smectite interlayer and relatively higher amounts of dissolved K in solution (i.e high K solution: K interlayer values) are distinguishable from smectites with higher amounts of K^+ in the

smectite interlayer and relatively lower amounts of dissolved K in solution (i.e low K solution: K interlayer values). In terms of reactivity, the two unaltered (group A) smectites of B11 and B23 are characterized by low K^+ solution: high K^+ interlayer ratios of >18.000 (Figure 18) whereby more K^+ is located in solution and not in the interlayer. Weakly altered smectite (group B) contain low to intermediate interlayer K^+ contents and K solution: high K interlayer ratios of ca. 3.000–50.000. In contrast, the most altered (group C) smectites are with high K interlayer content and low K solution: high K interlayer ratios (<10.000). The exception to this pattern is B12 bentonite of basic igneous origin, which contains the lowered amount of interlayered K. The above relationship highlights the general observation that the increase in smectite interlayer charge toward more negative values is generally accompanied by the adsorption of more K in the interlayer sites and the relative depletion of dissolved K^+ in solution.

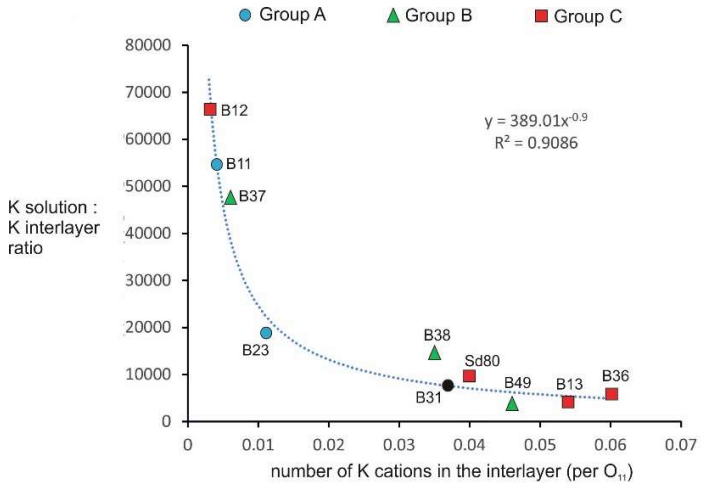

Figure 18: K-content in the smectite interlayer per half unit cell (O_{11}) plotted against the K solution (mg/l) : K interlayer (per O_{11}) ratio for ten of the bentonite samples after treatment with the saline cap solution at 120°C for 1 year. Solid point is B31, which could not be assigned to an alteration group due to the lack of a reliable layer charge determination

The relationship between smectite alteration and the pH of the reacted solution is also shown in Table 14. Only four of the saline cap rock solutions measured showed significant differences in pH from the original value of 7.3. These produced the more acidic solutions of the B11, B16, B36 and B37 bentonite batches with pH values ranging between 3.5 and 6. One possible cause of this acidity is the absence of carbonates combined with the presence of minor quantities of sulphide minerals (e.g. pyrite) in these samples that during partial oxidation are known to result in rapid acidification under hydrous conditions. The concentration of pyrite present often lies beneath the level of detection by XRD in these samples, but was detected by SEM study, for example, in the B16 Bayern bentonite. Whereas all of the bentonites characterized by acidic solutions underwent smectite alteration at temperatures of 120°C in the saline cap solution, it is also evident that significant changes in layer charge and metal substitution also occurred in neutral solutions.

Whereas a decrease in the pH of the solution can be expected to lead to more rapid dissolution of many mineral phases (e.g. carbonate minerals and feldspars), the increase in acidity does not appear to be a prerequisite for increased metal substitutions within the smectite lattice layers.

The best example is the SD80 Milos smectite that showed the highest degree of alteration in the tetrahedral layers with significant substitution of Si^{4+} by Al^{3+} and minor amounts of metal substitution of octahedral metals (Al^{3+} and $Mg^{2+}$by Fe^{3+}), all of which occurred in a close to neutral solution (pH 7.09). Similarly, higher degrees of smectite alteration were also seen in the neutral solutions of the B12, B13 and B19 bentonite batch experiments.

The above features indicate that extensive mineral dissolution can occur under neutral pH conditions and slightly alkaline conditions. This could be confirmed by SEM examination of the unreacted and reacted bentonite samples, whereby the dissolution of the smectite particles resulted in a smoother appearance to the textured mineral films, together with the more fragmentation and splitting of the clay mineral particles (Figure 9). That significant amounts of dissolution occurred at a neutral pH can be explained by consideration of published experimental studies on the role of pH and smectite dissolution. At elevated temperatures (e.g. 70 °C), the lowest rate of smectite dissolution has been known to shift toward more acidic conditions, with the lowest rate of dissolution occurring at a pH values of between 5 and 6 and with a higher dissolution rate at a pH of 7 (Rozalen et al. 2009).

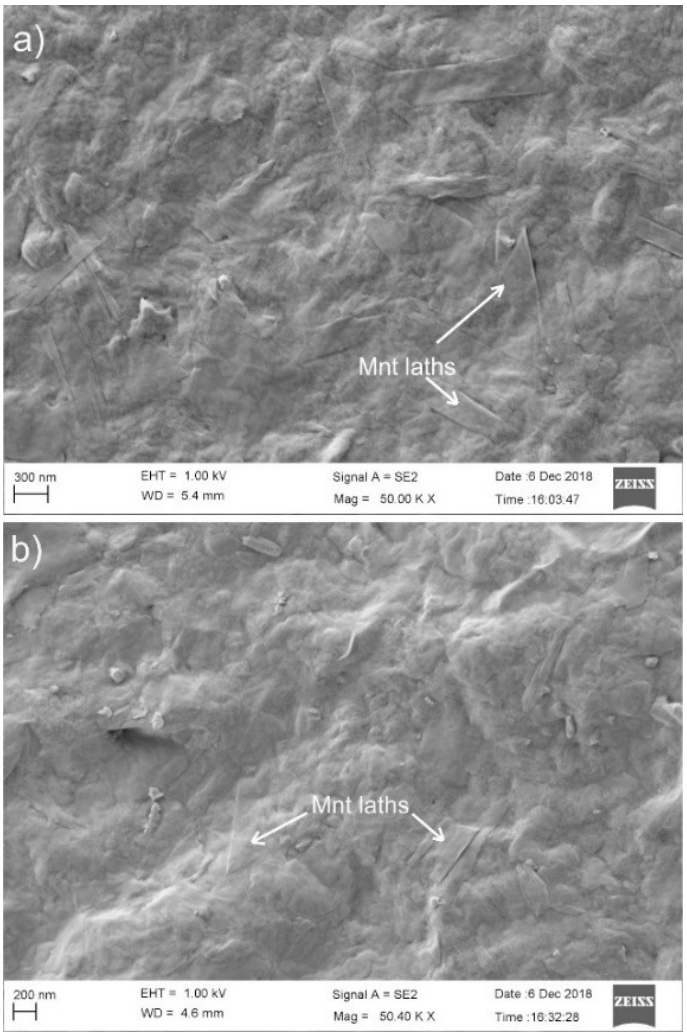

Figure 19: Smectite (montmorillonite) laths in the SD80 bentonite in a) its original state and b) after 1 year treatment in saline cap solution at 120°C. After treatment that lath surfaces appear slightly smoother and in part are fragmented due to possible dissolution. There is, however, no indication for re-precipitation of particles. Mnt = montmorillonite.

In order to determine whether the increase of interlayer K^+ was incorporated as illite layers within the smectite, the % illite content was determined by XRD following the principles outlined in Moore & Reynolds (1997) and the results summarized in Table 16. Although some illite layers (generally <10 %) occur in the natural smectite samples of the India Kutch bentonites of B10, B11 and B12 and in the B19, B31 and B49 bentonites, there was no clear indication of further illitization after experimentation that could be detected outside the range of the accuracy of the method (± 5 %). The change from 0 to 5 % illite layers observed following treatment of the B23 bentonite did not correspond with any change in the layer charge of the smectite in this sample and therefore the adsorption of fixed K^+ is considered to be unlikely. Due to the small changes in smectite layer charge observed in most of the bentonites studied and the lack of detectable illitization, the minor increase in the amount of interlayer K^+ observed in the 120 °C experiments with the saline cap solution is likely to be adsorbed as an exchangeable cation.

Table 16: *Estimation of interlayered illite content in smectite based on XRD study of ethylene glycolated unaltered and altered bentonites taken from the 120°C, 1 year series treated with the saline cap solution. The calculation of % illite layers is based on 003-002 reflection 2ϑ values as if measured using a Cu-anode (Moore & Reynolds 1997) and using a linear regression (%illite = 60.54 * 003-002 reflection in 2ϑ - 323.23). The accuracy for the estimation of % illite is ± 5.*

Sample	Source	unaltered	% illite (± 5)	120°C, 1 year	% illite (± 5)	Difference	Group
		003-002		003-002		Δ003-002	
B4	Milos, Greece	5.39	3	5.35	1	-0.04	B
B9	Wyoming*	5.28	0	5.26	0	-0.02	
B10	India, Kutch	5.47	8	-	-	-	-
B11	India, Kutch	5.46	7	5.43	6	-0.03	A
B12	India, Kutch	5.38	2	5.36	1	-0.02	C
B13	Hungary	-	-	5.39	3	-	C
B16	Bayern	5.26	0	5.34	0	+0.08	C
B19	Almeria, Spain	5.51	11	5.50	10	-0.01	C
B23	Argentina	5.32	0	5.42	5	+0.10	A
B31	Armenia*	5.44	7	5.40	4	-0.04	-
B36	Slovakia, Liskovec	5.28	0	5.37	2	+0.09	C
B37	Slovakia, Jelsovy Potok	5.26	0	5.28	0	+0.02	B
B38	Russia	5.28	0	5.41	4	+0.13	B
B49	Balekesir, Turkey*	5.50	10	-	-	-	B
SD80	Milos, Greece	5.34	0	5.31	0	+0.03	C

6 Conclusions and research outlook

1) From the 15 bentonite samples studied all showed a high degree of smectite stability in saline cap solution or Opalinus clay solution (fluid : bentonite ratio of 2:1) when treated in batch reactors at 25°, 60° and 90°C over a reaction time of up to 2 years. Only cation exchange reactions were recognizable in the smectite interlayers. Cation exchange was most evident in the saline cap solution with increased adsorption of Ca^{2+} observed in most bentonite samples of the bentonites. The precise concentrations of interlayer cations was also influenced by mineral dissolution of the complex bentonite assemblages, with adsorption of K^{+} ions in the more altered smectite (e.g. B36) and relative depletion of dissolved K^{+} in solution.

2) Varying degrees of tetrahedral and octahedral metal substitution leading to higher negative layer charges occurred in most of the bentonite samples after 120°C batch treatments, in particular in the more reactive saline cap solution. These reactions occurred without the nucleation and growth of new smectite phases. Only two Na-bentonites (B11- India, Kutch and B23, Argentina) showed no metal substitutions and appear to contain the most stable smectites under the conditions tested. In contrast, the most altered smectites were Ca-bentonites although there is no obvious relationship between the crystal-chemical characteristics of these smectites (e.g. layer charge or composition) and the degree of alteration observed.

3) The addition of organic substrates to the batch solutions for enhancing microbial activity did effect the types of cation exchange occurring in the smectite interlayers but there were no recognisable metal substitution in tetrahedral or octahedral sites and no total layer change changes that could be attributed directly to such activity.

4) Further research is required to constrain the reaction rates of the smectite alteration recognized in these experiments so that long-term states can be better predicted. The controlling factors of the metal substitutions occurring is still not clarified and requires experiments using bentonite mineral mixtures of lower complexity. The role of mineral-bacteria interactions is also an aspect that requires further study.

7 Acknowledgements

We thank Markus Peltz for help with the EDX determinations, Robert Mrotzek and Manfred Zander for their technical support in the laboratory and Arek Derkowski, from the Polish Academy of Science in Krakow for supporting the OD data collection of Inga Nietiedt. Stephan Kaufhold (BGR) and Holger Bittdorf (PTKA-WTE) are thanked for their continuous support and help throughout the project.

8 References

Berkowitz, B., Singurindy, O., Lowell, R.P. (2003). Mixing-driven diagenesis and mineral deposition: CaCO3 precipitation in salt water – Fresh water mixing zones. Geophysical Research Letters, 30 (5), 1253.

Christidis, G. (1998). Comparative study of the mobility of major and trace elements during alteration of an andesite and a rhyolite to bentonite in the Islands of Milos and Kimolos, Aegean, Greece. Clays and Clay Minerals, 46, 379-399.

Doebelin, N., Kleeberg, R. (2015). Profex: a graphical user interface for the Rietveld refinement BGMN. Journal of Applied Crystallography, 48, 1573-1580.

Grathoff, G.H., Podlech, C., Warr, L.N., Meleshyn, A. (2018). The stability of bentonites in aqueous solutions (25 to 120°C) relevant to the underground sealing of radioactive waste deposits, 9th MECC Conference, 17-21 September 2018 in Zagreb, Croatia – Poster abstract

Herbert, H., J. Kasbohm, J., Nguyen T. Lan, Meyer, L., Hoang Thi Minh Thao., Xie, M. (2011). Fe-Bentonite - Experiments and Modelling of the Interactions of Bentonites with Iron.- GRS-295, ISBN 978-3-939355-72-4, GRS Braunschweig.

Kuligiewicz, A., Derkowski, A., Emmerich, K., Christidis, G.E., Tsiantos, C., Gionis, V., Chryssikos, G.D. (2015). Measuring the layer charge of dioctahedral smectite by O-D vitrational spectroscopy. Clays and Clay Minerals, 63, 443-456.

Kaufhold, S., Dohrmann, R., Koch, D., Houben, G. (2008). The pH of aqueous bentonite suspensions. Clays and Clay Minerals, 56 (3), 338-343.

Kaufhold, S., Dohrmann, R. (2010). Stability of bentonites in salt solutions II Potassium chloride solution – Initial step of illitization? Applied Clay Science, 49, 98-107.

Kaufhold, S., Dohrmann, R. (2011). Stability of bentonites in salt solutions III. Ca-hydroxide solutions. Applied Clay Science, 51, 300-307.

Kaufhold, S., Dohrmann, R. (2016). Distinguishing between more or less suitable bentonites for storage of high-level radioactive waste. Clay Minerals, 51, 289-302.

Le Bas, M.J., Le Maitre, R.W., Streckeisen, A., Zannettin, B. (1986). A chemical classification of volcanic rocks based on the total alkali-silica diagram. Journal of Petrology, 27 (3), 745-750.

Manzel, T. (2019): In Situ Messunge n des Quellverhaltens von Bontonit in Nasszellen durch Röntgendiffraktometrie Bachelor Arbeit Universität Greifswald, 33 p.

Matschiavelli, N., Drozdowski, J., Kluge, S., Arnold, T., Cherkouk, A. (2019). Joint Project: Umwandlungsmechanismen in Bentonitbarrieren, Subproject B: Einfluss von mikrobiellen Prozessen auf die Bentonitumwandlung, Wissenschaftlich-Technische Berichte, HZDR-103, ISSN 2191-8716 http://www.hzdr.de/publications/Publ-29398

Meier, L.P., Kahr, G. (1999). Determination of the cation exchange capacity (CEC) of clay minerals using the complexes of copper(II) ion with triethylenetetramine and tetraethlyenepentamine. Clays and Clay Minerals, 47, 386-388.

Meleshyn, A. (2019). Carbonate dissolution, CO2 release, swelling behaviour, and permeability of 15 bentonites upon reaction with a highly saline water and a brine at 25, 90, and 120°C: Mechanisms of transformation of bentonite barriers (UMB). Report GRS-547, GRS gGmbH, Braunschweig.

Moore, D.M., Reynolds, R.C. Jr. (1997). X-ray diffraction and Identification and Analysis of Clay Minerals, 2nd Edition, Oxford University press, pp 378.

Nietiedt, I.M. (2019). Mineralogie: Bestimmung der Schichtladung von Bentoniten mittels FTIR-Spektroskopie. Unpublished B.Sc report, University of Greifswald, pp. 14.

Kuligiewicz, A., Derkowski, A., Emmerich, K., Christidis, G.E., Tsiantos, C., Gionis, V., Chryssikos, D. (2015). Measuring the layer charge of dioctahedral smectite by O-D vibrational spectroscopy. Clays and Clay Minerals, 63, 443-456.

Olsson, S., Karnland, O. (2009). Characterisation of bentonites from Kutch, India and Milos, Greece – some candidate tunnel back-fill materials? SKB Rapport R-09-53, pp 35.

Podlech, C., Grathoff, G.H., Warr, L.N., Kasbohm, J. (2016). The stability of bentonites and saponitic clays in aqueous solutions relevant to the underground sealing of radioactive waste deposits.; 53th CMS meeting, 5-8 June 2016, Atlanta, Georgia, USA – Poster abstract

Podlech, C., Grathoff, G.H., Kasbohm, J., Warr, L.N. (2017). Advances in quantifying smectite composition by TEM-EDX mapping with applications for monitoring bentonite alteration. 54th CMS meeting, 2-8 June 2017, Edmonton, Alberta, Canada – Poster abstract

Podlech, C., Matschiavelli, N., Grathoff, G.H., Warr, L.N. (2018). Bentonite alteration in aqueous solutions relevant to the underground disposal of radioactive waste including the effects of microbial activity.; 55th CMS meeting , 11-14 June 2018, Champaign, Illinois, USA – Talk, abstract http://conferences.illinois.edu/cms/docs/CMS%202018%20Program%20&%20Abstracts%20June11.pdf

Ufer, K., Stanjek, H., Roth, G., Dohrmann, R., Kleeberg, R., Kaufhold, S. (2008). Quantitative phase analysis of bentonites by the Rietveld method. Clays and Clay Minerals, 56 (2), 272-282.

Rozalen, M., Brady, P., Huertas, E.J. (2009). Surface chemistry of K-montmorillonite: Ionic strength, temperature dependence and dissolution kinetics. Journal of Colloid and Interface Science, 333, 474-484.

Shah, N.R. (1997). Indian bentonite – focus on the Kutch region. Industrial Minerals, 359, 43-47.

Small, J.S. (1994). Fluid composition, mineralogy and morphological changes associated with the smectite-to-illite reaction: An experimental investigation of the effect of organic acid anions. Clay Minerals, 29, 539-554.

Köster, H.M. (1977). Die Berechnung kristallchemischer Strukturformeln von 2:1-Schichtsilikaten unter Berücksichtigung der gemessenen Zwischenschichtladungen und Kationenumtauschkapazitäten, sowie die Darstellung der Ladungsverteilung in der Struktur mittels Dreieckskoordinaten. Clay Minerals, 12, 45-54.

Hoang-Minh, T., Kasbohn, J., Nguyen-Thanh, L., Thi Nga, T., Thi. L., Thuy Duong, N., Duc Thanh, N., Thi Minh Thuyet, N., Duy Anh, D., Pusch, R., Knutsson, S., Mählmann, R.F. (2018). Use of the TEM-EDX for

structural formula identification of clay minerals: a case study of Di Linh bentonite, Vietnam. Journal of Applied Crystallography, 52, 133-147.

Warr, L.N., Berger, J. (2007). Hydration of bentonite in natural waters: Application of „confined volume "wet-cell X-ray diffractometry. Physics and Chemistry of the Earth, 247-258.

Warr, L.N., Perdrial, J.N., Lett, M-C., Heinrich-Salmeron, A., Khodja, M. (2009). Clay mineral-enhanced bioremediation of marine oil pollution. Applied Clay Science, 46, 337-345.

Warr, L.N., van der Pluijm, B.A., Hofmann, H. (2016). Constraining the alteration history of a Late Cretaceous Patagonian volcaniclastic bentonite-ash-mudstone sequence using 40K/40Ar and 40Ar/39Ar isotopes. International Journal of Earth Sciences, 106 (1), 255-268.

Warr, L.N., Podlech, C., Grathoff. G, Kaufhold, S. (2018). The role of accessory minerals on the stability of the bentonite backfill. 2-6 September 2018, Bonn, Germany. Talk abstract. http://www.geobonn2018.de/assets/geobonn_2018_abstracts_12092018.pdf

9 Appendix A (electronic)

- Excel database of all analyses
- Jörn Kasbohm - Consulting reports (2015 & 2018)
- Layer charge report (Nietiedt 2019)
- Bachelor Arbeit von Tobias Manzel (Manzel 2019)
- Powerpoint presentations (Podlech 2016-2018)